

AUTOMATED CONTROL OF CZOCHRALSKI AND SHAPED CRYSTAL GROWTH PROCESSES USING WEIGHING TECHNIQUES

Nikolai V. Abrosimov^{1,2}, Vladimir N. Kurlov^{1,*} and
Sergei N. Rossolenko¹

¹ *Institute of Solid State Physics, Russian Academy of Science, Chernogolovka,
Moscow distr., 142432, Russia.*

² *Institute of Crystal Growth, Max-Born-Str. 2, D-12489 Berlin, Germany*

Contents

1. Introduction	2
2. Main features of controlling software	3
2.1. Main functions of growth programs. Program operators	4
2.2. Time sequence of program operators functioning	5
3. Automated control of oxide crystal growth by the conventional Czochralski technique	7
3.1. Calculation of programmed mass according to preset crystal shape	7
3.2. Estimating the state vector of the controlled object	14
4. Automated modified Czochralski technique using a plate in the melt	20
5. Automated modified Stepanov/EFG technique using capillary feeding of the plate above the melt	23
6. Automated Czochralski technique for semiconducting alloys	27
6.1. Segregation coefficient of minor component less than unity	27

* Corresponding author. Fax: ++007(096)5249701; E-mail: kurlov@issp.ac.ru

6.2. Segregation coefficient of minor component greater than unity	32
7. Automated shaped crystal growth	35
7.1. Edge-defined film-fed growth	35
7.1.1. Process of automated crystal seeding	38
7.1.2. Calculation of the programmed mass change for the tube enlargement	39
7.1.3. Calculation of the programmed mass change for the plate enlargement	43
7.1.4. In situ correction of the programmed mass change	44
7.1.5. Steady state growth	45
7.2. Non-Capillary Shaping (NCS) technique	47
8. Conclusions	52
Acknowledgements	52
References	53

1. Introduction

Modern crystal growth can not be imagined without computer based control systems used for monitoring the growth processes. In the case of crystal pulling from the melt the main part of such systems consists of the automated control of cross-section or diameter of the growing crystals. The driving force for development of automated control systems was the industrial production of oxides, semiconducting crystals (e.g. *Si*, *Ge*, $A^{III}B^V$) that required in improving the yield of the processes by raising reproducibility and minimizing cutting waste. The growth of many oxide crystals from the melt would practically not be possible without automated diameter control because of the extremely low growth rates and sensitivity to stabilization of the growth parameters during the long time. Automated control is also important to maintain the quality of the crystals and in the development of new technological processes.

A variety of different approaches for monitoring diameter, both direct and indirect, during Czochralski crystal growth are known, and a survey of the various techniques is given in [1, 2]. Techniques for automatic diameter control can be conveniently classified under the following headings.

1) Use of optical reflection from the meniscus [3-5]. The “bright ring” technique is particularly suited to the growth of silicon because of its large meniscus height.

2) Direct imaging of the crystal with use of a computer algorithm from which a measure of the current crystal diameter is obtained [6-8]. Optical, infra-red and X-ray imaging systems all have been developed.

3) The control of melt level with the use of a laser or electrocontact sensor. This control was successfully used for growth of bulk alkali halides crystals [9].

4) Weighing the crystal [1, 10–12] or the crucible [13, 14]. The use of a die for the control of the cross-section of the growing crystals is not sufficient for stable crystal growth and additional controlling systems, such as direct imaging of the crystal profile or meniscus height or weighing the crystal have to be used.

Of these, the weighing method is certainly the most versatile and the one most widely used.

The present review summarizes the long time experience of the authors in the development of process automatization by the growth of a wide range of materials (e.g. oxides, semiconducting alloys) by different modifications of Czochralski and shaped crystal growth techniques.

2. Main features of controlling software

The high level of modern automated processes of crystal growth from the melt requires an appropriate efficiency of the controlling software that take into account complexity of physical and chemical phenomena taking place during the growth. Software has to represent mathematical models of these phenomena and possibilities for their control. Crystal growers have to develop new growth techniques or deal with different materials and growth conditions. For this purpose it is necessary to modify construction of thermal zone of the crystal growth installation, structure and parameters of automated control system and, correspondingly, software structure. In this case the software quality depends on its capability to be adjusted to new growth techniques, materials and conditions. The higher the adaptation level, the more efficient is the growth software.

Since software should be applied to a wide range of technologies, it must allow relative universality. For software to be universal within a single class it should have some general structure and some elements typical for each process.

As is well known, any control program should read signals of the equipment sensors. Among the widely used sensors are crystal and/or crucible weight cells, thermocouples, sensors of heating power and translations and rotations of upper and lower drives and sensors of chamber vacuum and pressure. Then sensor data processing, trajectory and control effects calculation are carried out. After this control data generation output to the drives has to be performed. Drives include heaters, pulling and rotation mechanisms, etc. To direct process control a program includes a system of menus to start or finish necessary regimes and to make changes of parameters. The program must also produce the output of information via tables, graphics and file.

2.1. Main functions of growth programs. Program operators

The control program should directly control the process (to ask transducers, to calculate control actions and to transfer them to final-control devices), display information on the monitor, send it into a file, and also to input data if a user wants. More detailed analysis allows us to determine the following main functions in growth programs:

- calculation of mathematical functions;
- processing of numerical codes of transducer signals;
- calculation of control actions;
- transducer signal measurement;
- data output to final-control devices;
- periodic display of table rows on the monitor;
- data graphical presentation;
- periodic data output to the file;
- processing of the functional keyboard button;
- imaging of the process state-of- the art;
- input of the data.

We suppose that these functions are common for all growth programs. Apart from the common functions, programs related to definite methods of crystal growth can also have specific properties that could not be generalized. In different programs some general functions can be realized in different ways. Parts of a program, realizing some functions and referred to later as “program operators”, are grouped in special libraries. Procedures, parts of them, and their sets provide examples of program operators.

Thus a program controlling a particular method of crystal growth is somehow composed of appropriate program operators. The unified combination of the program operators reflects the structure of the control system and depends on the process and on the computer time characteristics. This combination is a common structural part of all growth programs, while other operator sets can vary from one program to another.

One can choose some of these operators from libraries and use them in programs only if they are realized according to a common standard. The array of general parameters, referred to later as the “dataway”, is entered for data exchange between operators. Operators use some elements of this dataway for reading and writing the parameter values.

All data used by program operators can be related to four types:

- (1) the parameters which are determined before the crystal growth and can be changed during the programming neither by a user nor by the program itself;

- (2) the parameters which can be redefined in the process of programming only by the user;
- (3) the parameters which can be changed only by the program itself;
- (4) the parameters which can be changed both by the program and by the user.

Parameters of the first type define the set of chosen operators and time sequence of the program functioning. It makes no sense to change these parameters in the growth process because of various transient uncontrolled processes. Parameters of the second type are constants defining the functions realized by operators. Parameters of the third type are inner operator variables necessary for their functioning. Data of the fourth type are in the parameter dataway and characterize the current state of the growth process.

2.2. Time sequence of program operators functioning

The basis of the combination of the program operator is their distribution over the available computing power. If the growth equipment has a distributed computing automated control system power, i.e., a network of some processors, the user should define which processor performs the particular operator group. For example a two-processor system can be realized. It means that measuring of transducer signals and data output to final-control devices are carried out in a special processor connected to external devices. Other operators are carried out in the processor of another computer.

In the case of single-processor computing system, the operators should be called periodically and the system successively executes them during the time interval τ determined by the total time of successive performing of all operators used by the program. To the extent that crystal growth processes are rather slow, i.e., their characteristic times are seconds or even minutes [15, 16], it is sufficient to have $\tau=1-10$ s. Operators can be accessed with any step period multiples of τ .

The user should have the possibility to begin and finish execution of any operator from the computer keyboard or another device for data input to influence some processes. Furthermore, the program operators should automatically start up and be completed in the case of some events.

Some arrays of events connected with the program operators in use represent input data. Furthermore, events connected with computation inside the program operators also constitute elements of the array. For example if some operator computes some variable defined by a piecewise linear function then, apart from this operation, one can define as an event the calculation of a section of this function. An event for some operator inside every step τ is defined by a logic combinations of all events in the current and also in all preceding steps. This expression can be rather complicated. Thus from all logic combination one chooses those for which events are analyzed in all the steps.

A system of logic expressions for all the chosen operators determines the time sequence of functioning of the control program. The program operator set and the corresponding logic expressions are responsible for the control program for the specified method of crystal growth.

To make the control program for a specified methods of growth means to describe it abstractly, i.e., to compile the program operator set and to construct the system of logic expressions.

Then, on the basis of this abstract description and by using a special Editor Program the operator set, logic expression system and initial parameter values are determined.

Usually, the program has to maintain several stages of the crystal growth processes:

- heating of the charge in the crucible and its melting;
- dipping of the seed into the melt or onto the shaper and start of pulling;
- crystal shaping;
- crystal pull off from the melt;
- crystal cooling.

Controlling software must have possibilities to make full automation via consequent executing the above stages of the processes and to make manual corrections at each stage and transitions from one stage to another.

A change of the heating power or temperatures of the thermal zone can be made in different ways: direct input of the appropriate value of heating power, step-wise change of heating power by pressing the functional keys on the keyboard and changing the heating power by a piece-wise linear function depending on time. The first way is used for the fast change of the power, e.g. in emergencies. The second way is used as a manual minor correction of power during automatic growth. The third way is applied, for example, during the charge heating or crystal cooling. It can be also used as an additional program changing method during automatic crystal shaping

Change of the rates of pulling and rotation of the crystal and crucible is realized in the same manner as for heating power change. Additionally, rates can change in a manner depending not only on time, but also on the length, radius and mass of the crystal. These additional changes are used at the stages of expanding and narrowing of the crystal. At these stages it is necessary to decrease (while the crystal is expanding) and to increase (while the crystal is narrowing) the pulling rate of the crystal depending on its radius. At the stage of stationary shaping, the rates of rotation of crystal and crucible should be changed depending on the length of crystal in order to stabilize a planar front of crystallization. In order to avoid constitutional supercooling during stationary growth the pulling rate is decreased with increase of crystal mass.

3. Automated control of oxide crystal growth by the conventional Czochralski technique

In the Czochralski technique the crystal grows from the meniscus formed on a free surface of melt onto the seed crystal of the required crystallographic orientation. The pull rod is lifted and rotated, and crystallization onto the end of the seed occurs (Fig. 1)

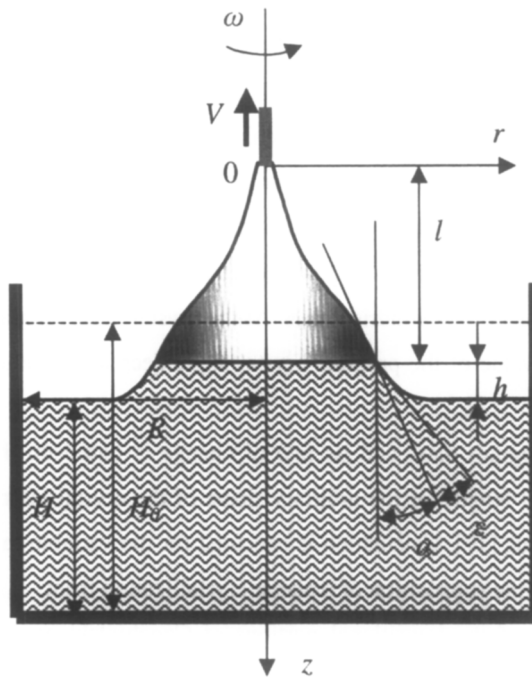


Fig. 1. Schematic illustration of growth parameters in the Czochralski process.

3.1. Calculation of programmed mass according to preset crystal shape

The main functions of a automated control system using a weight sensor in the Czochralski technique which are executing periodically at the necessary time intervals are the following:

1. Calculation of the programmed crystal shape which should be pulled.

2. Calculation of the programmed mass for the weight sensor according to the preset crystal shape and shape of the liquid meniscus.
3. Reading and filtering the real mass signal from the weight sensor.
4. Calculation of the deviation of the mass, its derivatives and, possibly, the first integral of the mass deviation.
5. Calculation of the controlling change of the heating power and pulling and rotation rates of the crystal and crucible using a proportional-integral-differential (PID), or some another, strategy.
6. Output of the control signals to the drivers.

In order to decrease the crystal radius or cross-sectional area overregulation at the stages of transition portions forming the crystal profile is described by the sufficiently smooth curves defined by the gradual change of the angle of the crystal enlargement (narrowing) [17]. During crystal enlargement the preset crystal angle grows from a minimal value at the neck formation (after dipping) up to a maximal value at half the radius of the cylindrical part and then decreases with further increase of radius. Transition to the cylindrical part is executed by some small angle and at a radius slightly smaller than the radius of the cylindrical part. At the crystal narrowing after formation of the cylindrical part the absolute value of the program crystal angle decreases gradually as a function of the decreasing crystal radius.

Calculation of the program mass and its rate of change is based on the calculation of the crystallization rate and crystal length for the arbitrary shape of the crystal taking into consideration the mass of the liquid meniscus [17]. Calculation is executed for the variable rates of crystal pulling and crucible translation under the supposition of a planar crystallization front.

Monitoring the shape of the transitional portions of Czochralski growing crystal is shown schematically in Fig. 2.

The expression for the crystallization rate of a crystal growing with the arbitrary shape can be produced as follows. It is known that at any time period of crystallization the angle between the tangent to the meniscus and the side crystal surface at a point on the three-phase line, termed the growth angle ε , is a constant in the isotropic approximation [18, 19]. The condition of constancy of the angle ε allows one to write the dependence of the crystal radius variation with time as

$$\dot{r} = V_c \operatorname{tg} \alpha, \quad (1)$$

$$\text{where } V_c = V_0 - \dot{H} - \dot{h} \quad (2)$$

is the crystallization rate equal to the rate of displacement of an arbitrary point on the crystal with respect to the solid-liquid interface, V_0 is the crystal pulling rate, \dot{H} is the rate of fall of the melt level in the crucible, \dot{h} is the rate of the meniscus height change.

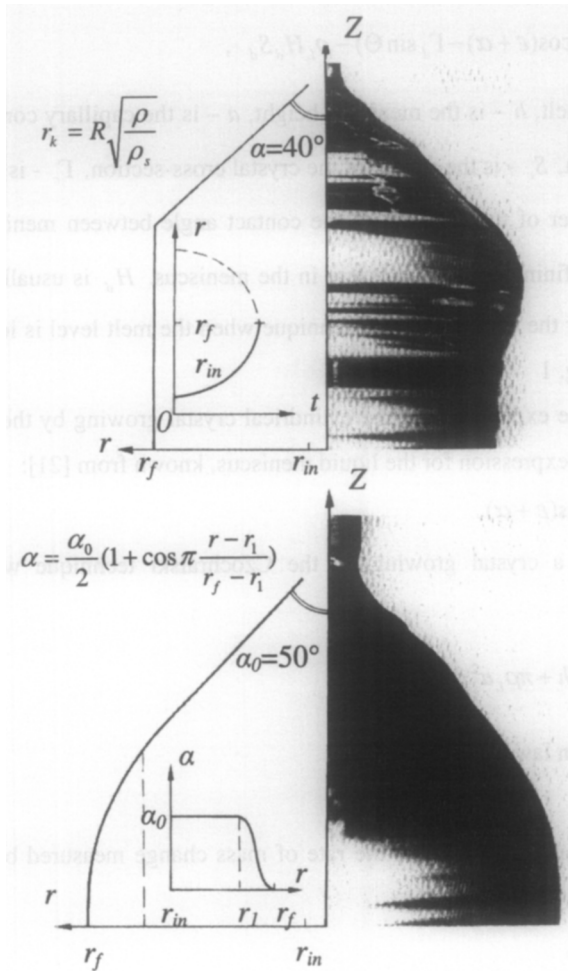


Fig. 2. a - Transitional portion of the $LiNbO_3$ crystal preset as a straight cone. The photograph of the crystal demonstrates overcorrection at the transition to the cylindrical portion caused by a thermal inertia of the growth process; b - Smooth decrease of the growth angle of the initial cone, beginning with a crystal radius r_1 , allows to avoid overcorrection at the transition to the cylindrical part of crystal.

Generally, for *Czochralski and Stepanov crystal growth techniques*, the mass recorded by the weight sensor is the sum of the solidified fraction, meniscus mass and influence of the external pressure on the meniscus. To calculate the programmed mass the expression for the meniscus mass and influence of the external pressure is obtained by integrating the Laplace capillary equation [20]. For arbitrary cross-section of the crystal it has the form:

$$M_m = \rho_L h S_c + \frac{1}{2} \rho_L a^2 (\Gamma_c \cos(\varepsilon + \alpha) - \Gamma_d \sin \Theta) - \rho_L H_d S_d, \quad (3)$$

where ρ_L is the density of the melt, h – is the meniscus height, a – is the capillary constant, S_d – is the square of the die cross-section, S_c – is the square of the crystal cross-section, Γ_c – is the perimeter of the crystal, Γ_d is the perimeter of the die, Θ – is the contact angle between meniscus and die, $H_d = H - H_0$ – is the constant defining external pressure in the meniscus. H_d is usually negative in the real crystal growth process by the Stepanov/EFG technique when the melt level is lower than the meniscus basis, as is shown in Fig. 1

Consideration of the above expression for the cylindrical crystal growing by the Czochralski technique results in the following expression for the liquid meniscus, known from [21]:

$$M_m = \pi \rho_L r^2 h + \pi \rho_L a^2 r \cos(\varepsilon + \alpha). \quad (4)$$

Thus, the total mass of a crystal growing by the Czochralski technique with a planar crystallization front is equal to:

$$M = \pi \rho_s \int_{t_0}^t r^2 V_c d\tau + \pi \rho_L r^2 h + \pi \rho_L a^2 r \cos(\varepsilon + \alpha). \quad (5)$$

From the mass conservation law follows:

$$\dot{M} = -\pi \rho_L R^2 \dot{H}. \quad (6)$$

Differentiating (5) yields an expression for the rate of mass change measured by the weight sensor:

$$\dot{M} = M'_t + (M'_r + M'_a \alpha'_r) \dot{r}, \quad (7)$$

where the corresponding partial derivatives have the form:

$$M'_t = \pi \rho_s r^2 V_c \quad (8)$$

$$M'_r = 2\pi \rho_L h r + \pi \rho_L r^2 h'_r + \pi \rho_L a^2 \cos(\varepsilon + \alpha) \quad (9)$$

$$M'_a = \pi \rho_L r^2 h'_a - \pi \rho_L a^2 r \sin(\varepsilon + \alpha). \quad (10)$$

The rate of the change of the melt level in the crucible can be written as:

$$\dot{H} = V_0 - V_c - (h'_r + h'_a \alpha'_r) V_c t g \alpha. \quad (11)$$

By solving equations (6) to (11) we obtain an expression for the crystallization rate:

$$V_c = \frac{\pi \rho_L R^2 V_0}{\pi \rho_L R^2 - \pi \rho_s r^2 + (\pi \rho_L R^2 (h'_r + h'_a \alpha'_r) - (M'_r + M'_a \alpha'_r)) t g \alpha}. \quad (12)$$

Note that, in the case of the constant-diameter crystal growth, $r = \text{const}$ or else $\alpha = 0$, expression (12) yields the known formula for the crystallization rate:

$$V_c = \frac{\rho_L R^2 V_0}{\rho_L R^2 - \rho_S r^2}. \quad (13)$$

The partial derivatives h'_r and h'_α entering into (8) to (12) can be determined with an accuracy sufficient for practical application using the formula of Tsivinskii [22] or Johansen [23].

Assuming the explicit form of the functions $\alpha(r)$ and $\alpha'(r)$ one can integrate equations (1) and (7) thus solving the problem of programmed assignment to form a “cone” of any desired geometrical shape. Thus the algorithm of the programmed growth of the “cone” is as follows: using finite differences we obtain the relationships for the programmed values at the i -th step of monitoring.

$$\alpha_i = \alpha(r_i) - \text{preset functions,}$$

$$V_{c,i} = V_c(r_i, \alpha_i) - \text{calculated from expression (12),}$$

$$\Delta r_i = \tau V_{c,i} \lg \alpha_i - \text{calculated from expression (1),}$$

$$\dot{M}_i = \dot{M}(V_{c,i}, r_i, d_i) - \text{calculated from expression (7),}$$

$$M_{i+1} = M_i + \tau \dot{M}_i,$$

$$r_{i+1} = r_i + \Delta r_i,$$

where τ is the step of the time integration interval. A similar algorithm can be constructed for automatic systems that use a melt level sensor also.

Several simple examples of the transitional portions of the lithium niobate crystals have been grown with constant pulling rate with the use of the above algorithm in an automatic system of crystal weight control. Fig. 2a shows the example of crystal shape with a preset straight cone having a constant aperture angle at the vertex, $2\alpha = \text{const}$. Dependence of the crystal radius $r=r(t)$ on time shown in this figure is strongly non-linear and close to a cubic parabola. Practically, it is rather difficult to obtain a smooth transition from a straight cone to a cylindrical portion of the crystal because of the stepwise change of the angle α from its conical value to zero at the cylindrical part. Thermal inertia of the crystallization process prevents such a step-wise transition. This difficulty can be overcome by gradually decreasing the cone tilt angle starting from some crystal radius r_l and finishing at a final radius r_f (usually the radius of the cylindrical part). One particular realization of a smooth transition from a straight cone to a cylindrical part of the crystal is shown in Fig. 2b.

The transitional regions of a more complicated configuration providing a smooth transition to the cylindrical part of the crystal can be obtained using, for example, a linear piece-wise dependence of the angle α on r . As is shown in Fig. 3a, the angle α first increases according to a linear function in order to form the “cone”. Then it decreases by linear function from a certain radius value up to the radius of the cylindrical part. When the angle is small enough a cylindrical part begins to form. Fig.

3b shows a shape of the final “cone” of a lithium niobate crystal. Final “cones” have been grown also with the use of a linear decrease of the conical angle with decrease of the crystal radius. A slight discrepancy between the experimental and calculated profile curves is due to errors in the PID control. It can be shown that, with one-channel control, the dynamical closed loop is to first order a static one and error in the maintenance of the non-linear profile change is inevitable.

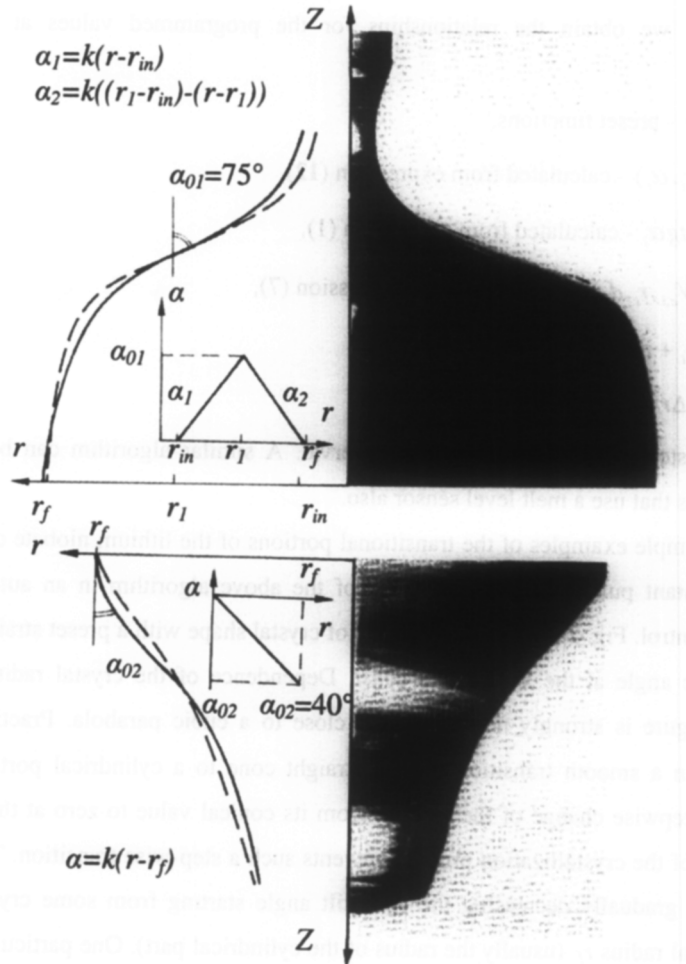


Fig. 3. a - Formation of the initial “cone” using the functions $\alpha_1 = \alpha_1(r)$ and $\alpha_2 = \alpha_2(r)$. The dashed line corresponds to the real profile curve of the crystal, shown in the right hand side of the figure; b - Reverse “cone” of the same crystal.

Assuming a smoother curve of $\alpha=\alpha(r)$ dependence one enables to reduce the control error during the formation of the transition portions of the crystal (Fig. 4).

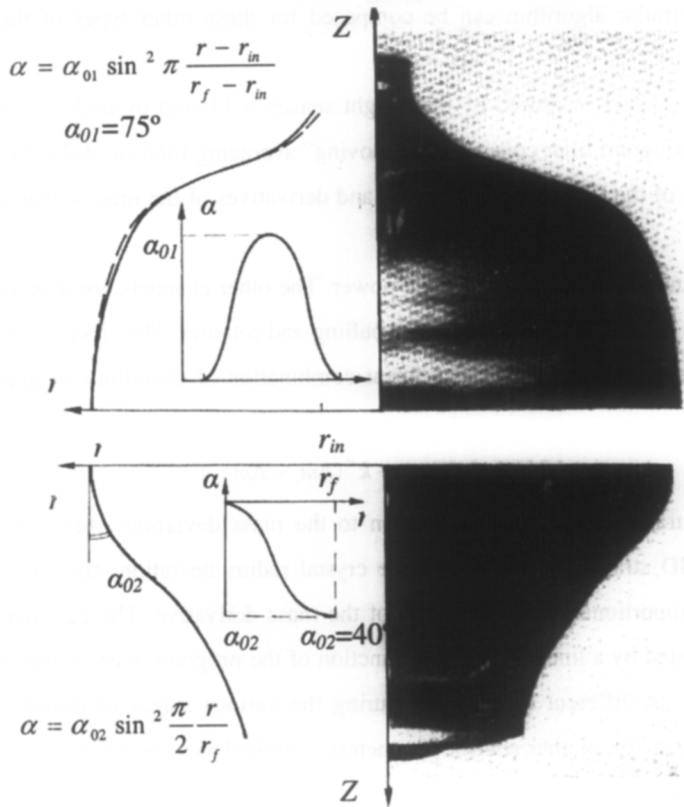


Fig. 4. Direct and reverse “cone” of a LiNbO_3 crystal. A smoother specified curve of the dependence $\alpha=\alpha(r)$ allows to reduce the error in monitoring the formation of the transitional regions of the crystal as compared with Figure 3.

Description of the shape of the growing crystal via the angle functions $\alpha(r)$ and $\alpha'(r)$ is not singular. Sometimes it is more convenient to describe dependences of the conical angle as the functions $\alpha(l)$ and $\alpha'(l)$ of the crystal length. In this case the expression for the non-stationary crystallization rate is:

$$V_c = \frac{V_0}{1 - \frac{\rho_s r^2}{\rho_L R^2} + (h'_r - \frac{m'_r}{\pi \rho_L R^2}) \text{tg } \alpha + (h'_\alpha - \frac{m'_\alpha}{\pi \rho_L R^2}) \alpha'_l} \quad (14)$$

It is possible to use only dependence of the radius $r(l)$ of the crystal on the length for a description of the preset shape of the crystal. In this case it is necessary to find first and second derivatives $r'(l)$ and $r''(l)$ of the function $r(l)$. Then, $r'(l)$ and $r''(l)$ should be used in the expression (14). A similar algorithm can be composed for these other types of the crystal shape description.

The true mass signal measured by the weight sensor is filtered by both active analogue and program filters. The program filter consists of a “moving” averaging filter or of the program analogue of an aperiodic chain of the first order. Deviations and derivatives of the mass signal are also filtered by program means.

The main channel of control is a heating power. The other channels, used as auxiliary means, involve changing the rates of crystal and crucible pulling and rotation. The changes of heating power or other control variables are calculated as a linear combination of deviations of mass, its first and second derivatives:

$$\Delta\rho_i = k^i(\Delta m_i - \Delta m_{i-1}) + k^p(\Delta \dot{m}_i - \Delta \dot{m}_{i-1}) + k^d(\Delta \ddot{m}_i - \Delta \ddot{m}_{i-1}). \quad (15)$$

So a PDD² strategy is realized in relation to the mass deviation which, in turn, is being implemented by a PID strategy in relation to the crystal radius deviation, since the crystal radius deviation is nearly proportional to the deviation of the mass derivative. The parameters of the PID regulator can be adjusted by a linear piece-wise function of the program mass change rate which can be markedly different at different crystal radii during the various stages of growth. The resulting change of heating power (or another control parameter) is limited to a certain value in order to avoid the influence of possible noise factors.

3.2. Estimating the state vector of the controlled object

As is known from theory [24], state regulators have some advantages over those which are developed for deviation of crystal mass. The state regulators can be used efficiently for unstable objects: to provide stability, it is required that feedback should be introduced with respect to several variables of state.

The first stage of practical synthesis of these regulators is the solving of the problem of estimating the control object state during the technological process. A similar problem of estimating the state was solved in [4] for an optical sensor of the bright ring surrounding the meniscus, used in silicon crystal growth.

In the Czochralski technique by the control object we mean a “melt-crystal” system, and as a state vector x is taken an extended vector with components: real crystal radius r , meniscus height h

and the associated values: flare angle α , crystal length l and melt level H in the crucible. The source of indirect information on the process of growth is the crystal weight sensor.

The problem of the estimating the state vector of the “melt-crystal” system from the weight signal is the inverse problem to the determination of the program mass according to the preset shape of the crystal which was described above.

The state vector can be determined by solving the weight sensor observation equation [25]. The problem is solved with the assumption that there exists a planar melt-crystal interface. The expression for the mass, M , measured with a weight sensor should be written in such form:

$$\pi\rho_s \int_{l_0}^l r^2(z)dz + \pi\rho_L r^2(l)h + \pi\rho_L a^2 r(l) \cos(\varepsilon + \alpha) = M(l). \quad (16)$$

The length l of the growing crystal is determined as follows:

$$l = l_s - h - H, \quad (17)$$

here $l_s = \int_{t_0}^t V_0(\tau)d\tau$ is the amount of translation of the pulling head. From the law of conservation of

mass in the absence of feeding the melt with charge we have:

$$H = -\frac{M - M_0}{\pi\rho_L R^2} + H_0. \quad (18)$$

The crucible radius $R=R(H)$ may be not constant, generally, and is defined as a function of the initial melt level. The quantities l_0 , M_0 , and H_0 are the initial values of the functions $l(t)$, $M(t)$ and $H(t)$ (at the moment of time $t=t_0$). The functions $V(t)$ or $l_s(t)$ are assumed to be known.

For the crystallization process, with an assumption of the existence of the angle of growth, ε , we may write [18]:

$$\alpha = \arctan r'_z, \quad z=l \quad (19)$$

$$h = h(r, \varepsilon + \alpha). \quad (20)$$

If melting occurs (which may take place during the growth process), the crystallization rate $V_c < 0$, and relation (19) does not hold [18]. However, in this case the crystal profile $r=r(l)$ and h are known, and the expression for

$$\varepsilon + \alpha = f(h, r) \quad (21)$$

is found from the approximated Laplace equation [26]. At the beginning of the crystal growth process the parameters of the seed are known:

$$r|_{l=l_0} = r_0, \quad (22)$$

$$\alpha|_{l=l_0} = \alpha_0. \quad (23)$$

Rectangles mark calculation of the corresponding expressions. In the left-hand side of the diagram one can see formation of program values of the vector x_p and mass m_p for a given crystal shape $r(l)$, according to equations (16)–(20). An approximate expression for the meniscus height h can be found in [22, 28, 29] and the crystallization rate V_c should be calculated using expression (14). In the right-hand side of the block-diagram in Fig. 5 the real values of the vector x are determined. The technique of successive approximations has been used for calculating these values. This technique can be reduced to correcting the radius r at each iteration step in accordance with the error δM of the mass M_r , measured by the weight sensor in response to the calculated one M_p . The real value of the radius $r_{r,i}$ at the i -th iteration step, is thus calculated as follows :

$$r_{r,i} = r_{r,i-1} + k\delta M, \quad (24)$$

here k is the weighing coefficient affecting the convergence of the calculation process. This coefficient is chosen so as to provide adequate convergence of the numerical calculation at all stages of the crystal growth process. The real values l_r , α_r , h_r , H_r are found according to equations (16)–(21).

Since the values of the mass M_r , measured during the process of growth by the weight sensor, are affected by a stochastic component of the signal, the iteration processes do not converge in some cases. To guarantee reliable convergence of numerical calculation, we used smoothing of the real shape function $r_r(l_r)$ by a one-dimensional spline or averaging $\alpha_r(l_r)$ with respect to several points. It should be noted that determination of r_r and α_r from equations (24) and (19) is valid only for the crystallization ($V_c > 0$) according to the given block-scheme of the calculation process. In the case of melting ($V_c < 0$) we do the following. The shape $r_r(l_r)$ has already been calculated and is known, for the value of r_r found on this curve and the calculated value of h_r , the angle $\alpha_{r,i}(r_{r,i}, h_{r,i-1})$ is determined from the expression derived in [26]. Further calculations are performed by analogy with the process of crystallization ($V_c > 0$).

To calculate the program vector x_p and program mass M_p in the shape transition regions, it is reasonable to use the real value l_r of the crystal length instead of the program length l_p (see dotted line in Fig.5 denoting Δl addition to l_p). Taking into account the real crystal length in automated control system during shaping the non-cylindrical crystal figures of rotation increases the accuracy and quality of the crystal shape control.

To compare numerical and experimental results, lithium niobate crystals of 80 mm diameter have been grown by the standard technique described above (Fig. 6). The crystals were grown in the $[10\bar{1}4]$ direction from a Pt crucible using crystal growth equipment with RF induction heating, in an air atmosphere. During the initial stage of growth the crystal pulling rate was 5 mm/h, at the end of the cone shaping and at the cylindrical part it was 2.5 mm/h, the rotation rate varying from 12 to 8 rpm.

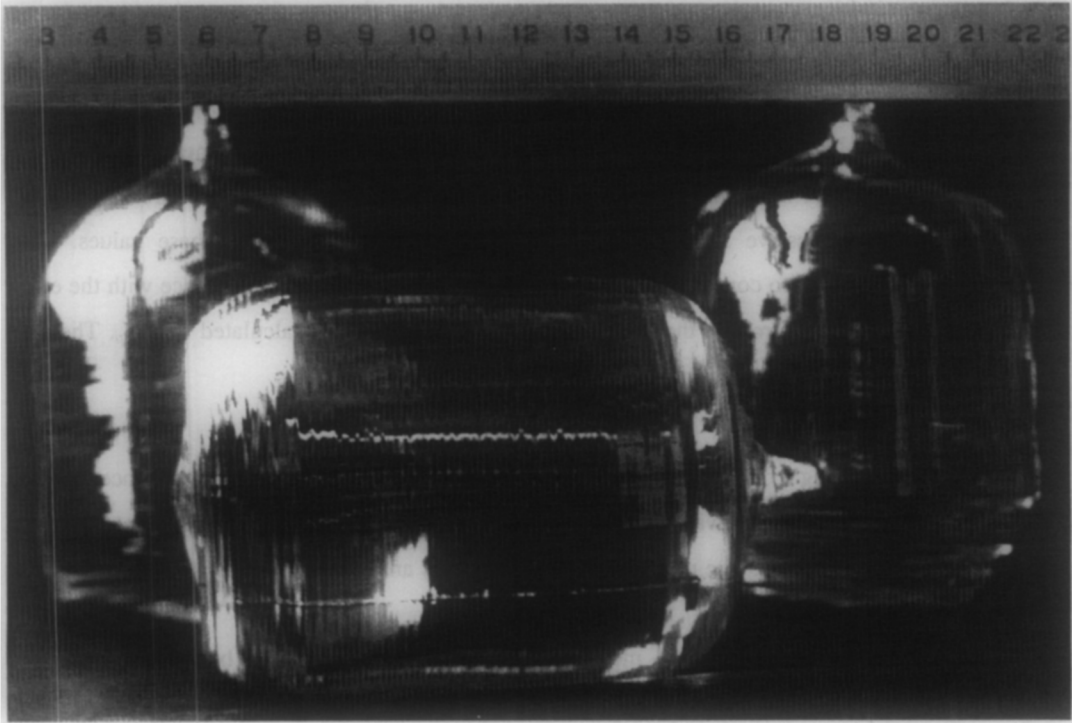


Fig. 6. Lithium niobate crystals of 80 mm in diameter.

During the growth at the stage of cylindrical portion shaping, the heating power was increased in a step-wise manner. This resulted in an increase of temperature in the crystallization zone and in a narrowing of the crystal. For part of the time the crystal diameter regulator was switched off. When it was achieved that the growing crystal mass deviated from the given one by several tens of grams, the regulator was switched on again, and the crystal was again withdrawn to the preassigned diameter. The transition process described is shown in Fig. 7.

The same figure presents graphs of experimental (solid line) and calculated (dotted line) transition processes of $r_r(l_r)$. The deviation of the calculated curve from the experimental one may be due to the dead zone of the weight sensor, to the temporal delay of the program filter and also to the errors in calculating the radius r_r .

Fig. 8 shows the graphs of deviations $\Delta l(l_r)$, $\Delta r(l_r)$, $\Delta \alpha(l_r)$, $\Delta h(l_r)$ depicted for the whole experimental process of the crystal growth.

These curves were calculated by the proposed technique for all values of the mass M , obtained from the weight sensor. The deviation for each value of $M_{r,j}$ (here j is the number of the element of

array M_r) was calculated until the error δM became sufficiently small. For instance, $|\delta M|_{\min} = 10^{-4}$ g, corresponded to the radius calculation error $|\delta r|_{\min} = 10^{-5}$ mm. In this case the number of calculation iterations, N , was varied for different stages of crystal pulling. At the beginning of the crystal growth ($r_p = 3$ mm), N was within the range 100–300, whereas at the stage of shaping of cylinder ($r_p = 40$ mm), N varied from 10 to 30. A decrease of the number of iterations, N , with increasing radius r_p is related to a decrease in the relative deviation of the mass change rate, $\Delta \dot{M} / \dot{M}_p$ (\dot{M}_p is the program rate of mass change).

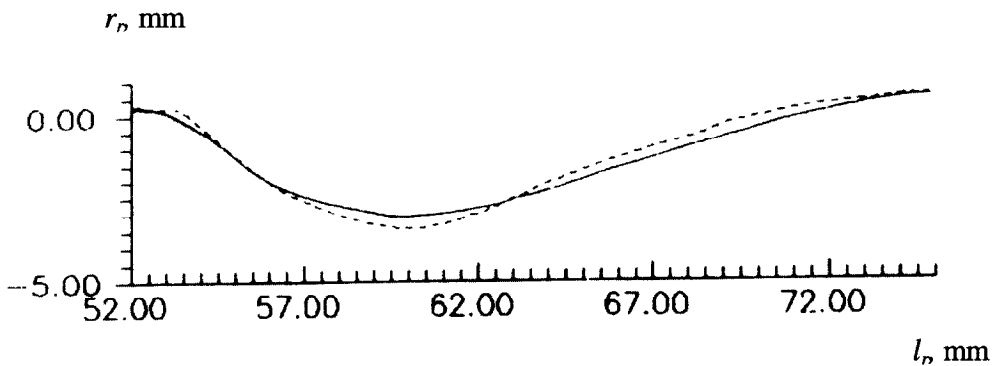


Fig. 7. Transition process at the surface of a lithium niobate crystal.

The anomalous behaviour of the curves in Fig. 8 at the section corresponding to 50–80 mm length is caused by an experimental step-wise increase of the heating power. The stepwise change of these curves at the final stage of crystal growth can be accounted for by transition of the control program to shaping of an inverse “cone”. The initial sections of the curves (up to the length $l_r = 38$ mm) refer to the stage of crystal expansion, performed according to the algorithm described above. Large errors in control at this stage corresponding to the maximal deviations Δl , Δr , $\Delta \alpha$, Δh refer to the relatively large angles of flare, $\alpha_p = 60\text{--}75^\circ$.

The developed technique of estimating the state of the control object during the crystal growth process has been very beneficial for the crystal growth control system. The information gained during the growth process can be used for synthesizing the state regulators. Besides, it has become possible to produce a display image of the state of the “melt-crystal” system. This enables growers to observe the dynamics of the growth process both by deviation of mass and its derivatives and by variation of the quantities with a clear physical sense, such as crystal radius, meniscus height, angle of crystal profile and so on. The approach developed can be used in the growth of various oxide crystals by Czochralski and Stepanov/ EFG techniques.

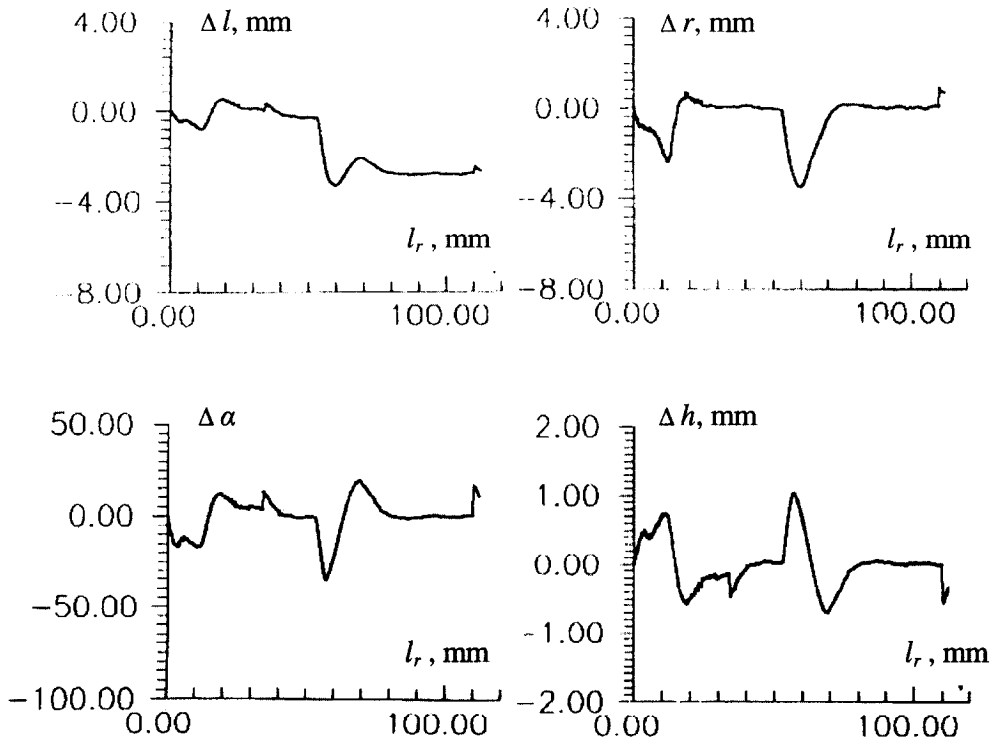


Fig. 8. Graphs of deviations Δl , Δr , $\Delta \alpha$, Δh obtained in the process of lithium niobate crystal growth.

4. Automated modified Czochralski technique using a plate in the melt

One of the main problem during the growth of crystals with non-circular (quadratoïd or rectangular) cross-section is the loss of growth stability [30]. For example, growth of high-quality rare-earth molybdate crystals along the [001] direction with constant cross-section by the conventional Czochralski technique is rather complicated and it is difficult to automate because the (100) and (010) faces fail to grow in a stable manner. The loss of growth stability is shown by the appearance, in the centres of the (100) and (010) faces, of non-faceted regions which deepen with growth, Fig. 9.

The mathematical simulation of evolution of the cross-section of crystals, having a 4-th order rotational symmetry axis, as a function of the angle growth anisotropy and solid-liquid interface

confirmed the experimental results [31]. It has been shown that it is necessary to achieve a planar or slightly convex interface and not to permit it to have concave form.



Fig. 9. Cross-section of a $Gd_2(MoO_4)_3$ crystal grown by the conventional Czochralski technique in the [001] direction.

The modified Czochralski technique using a plate in the melt was developed (Fig. 10) to maintain the crystallization front planar or slightly convex to the melt to increase the stability of the shape of the non-circular cross-section. For this purpose a metallic (*Pt*) planar plate should be immersed at a depth of some millimetres into the melt. This plate should be translated in the course of the process to maintain the distance between crystallization front and the plate constant or changing in accordance with a specific function.

Two problems can occur under these conditions. The first one is related to the low mechanical stability of the non-circular liquid meniscus. The second one is that the crystallization front may be contacted by the plate. To avoid these problems at the initial stage of the growth, the crystal is caused to expand at a large angle. There exists a narrow band of expansion angles and adjusting parameters of the automated system that produce a stable and non-contacting plate liquid meniscus. The crystal shape during the expansion stage is described by the piecewise linear dependence $r(l)$ of radius on length. Relatively large angles of crystal expansion prevent the transformation of the circular cross-

section to a quadratoid at this stage. A quadratoid cross-section shaping begins only at the stage of stationary growth.

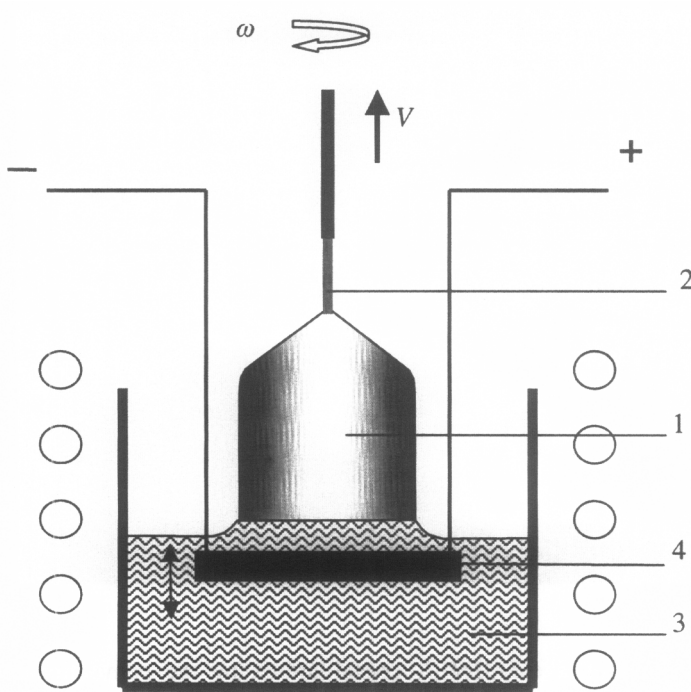


Fig. 10. Schematic illustration of modified Czochralski technique using plate in the melt. 1 - crystal; 2 - seed; 3 - melt; 4 - plate.

It is possible to consider the distance between crystallization front and a plate as a regulating parameter and to change this distance in response to deviation of the weight signal. In this case the plate acts as an additional local thermal factor, responding more rapidly in comparison with the usual heating from the crucible wall and influencing the thermal field in the area of the crystallization front. In our case a thermal zone was constructed so that the decrease of the plate immersing rate resulting in the decrease of the distance between the front crystallization on the plate produced a decrease of the temperature near the front of crystallization and increase of the crystal cross-section. The opposite situation was for the increase of the plate immersing rate which was equivalent to the heating power increase and resulted in the decrease of the crystal cross-section.

An electric current running through the plate immersed into the melt was used also as the local thermal regulating channel due to the Joule heat produced by the electric current. This technique acts like a changing immersing rate of the plate described earlier.

Using the technique described in this section, gadolinium and terbium molybdate single crystals with a maximum transverse cross-section of 30 mm have been grown. Gadolinium molybdate crystals grown with the use of the modified Czochralski technique are shown in Fig. 11.



Fig. 11. Gadolinium molybdate crystals with a maximum transverse cross-section of 30 mm grown with use of modified Czochralski technique.

5. Automated modified Stepanov/EFG technique using capillary feeding of the plate above the melt

This technique is somewhat similar to the above described modified Czochralski technique (see chapter 4). In this case the platinum plate keeping stable the crystallization front is located not in the melt, but above the melt surface providing capillary feeding of the plate and the crystal by the

crystallization is small enough at the small dimensions of the crystal, and there is no contact between the crystal and the plate.

To produce high quality $R_2(MoO_4)_3$ by this method, as has been shown experimentally, it is necessary that the pressure in the menisci should be constant during the crystal growth. This can be achieved by movement of crucible or die and both crucible and die simultaneously. During the growth of the $R_2(MoO_4)_3$ crystals the rate of movement of crucible or die was equal to the rate of decrease of melt level in the crucible and was defined using a system of automatic weight control of the growing crystal.

The modified Stepanov technique allows one to grow smooth transitional portions of the crystals as it was achieved in the growth of lithium niobate crystals by the Czochralski technique.

The temperature channel as well as the weight channel is connected with power change and changes of translation and rotation of the crystal and/or crucible. The programmed temperature of the thermocouple is usually described by several pieces of linear dependence on the crystal length. The gadolinium molybdate crystal grown with use of modified Stepanov/EFM technique is shown in Fig. 13.

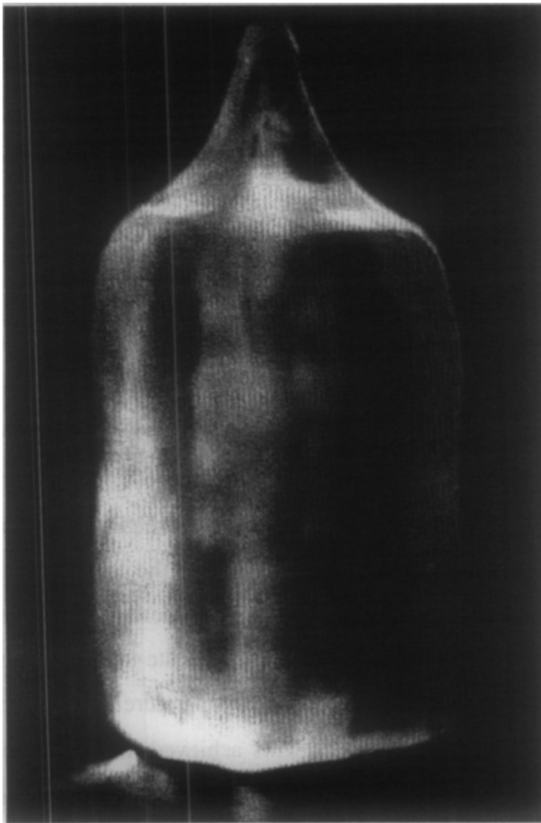


Fig. 13. Gadolinium molybdate crystal of $30 \times 30 \text{ mm}^2$ in cross-section grown by the modified Stepanov technique.

Fig. 14 shows the cross-sections of crystals grown at various rotation rates. It is seen that, with increasing rotation rate, the faceted crystal appears as if it were deformed but, in fact, no changes occur in crystallographic orientation.

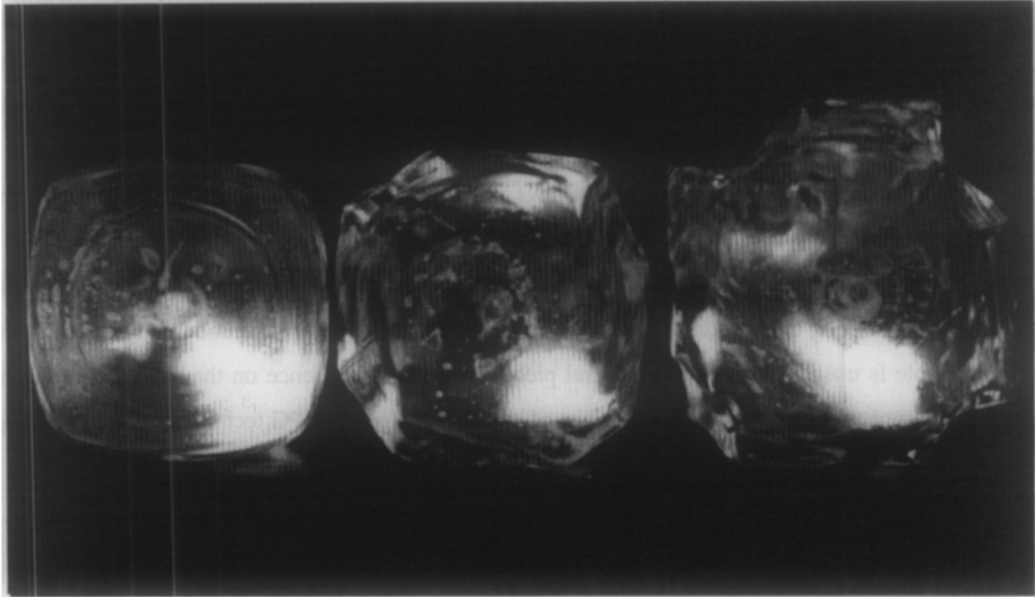


Fig. 14. Cross-section of $Gd_2(MoO_4)_3$ crystals grown by the modified Stepanov technique with various rotation rates: 20 rpm (on the left); 60 rpm (on the middle); 100 rpm (on the right).

A programmed dependence of temperature on length for this crystal was defined by two linear pieces of the 30 mm length. Their slopes were 0.13 and 0.17 grad mm^{-1} , respectively. A PID law was used for the heating power change connected with temperature deviation. By using a plate temperature channel of heating power control the amplification coefficient in the weight channel was decreased approximately five fold in comparison with one that was used at the stage of crystal expansion realized without use of plate temperature. Thus the influence of the weight channel was decreased but it was not fully switched off in order to maintain a preset shape of the crystal. By this, an error in weight control and consequently in shape control was increased but there was no contact of the crystallization front with the plate. The error in the maintenance of the plate temperature was not more than 7° , that is nearly 0.7% related to the minimum value of the temperature measured by a thermocouple during the whole process of crystal pulling (1020°). This achieved minimal error is comparable with a thermocouple error measuring the temperature. Temperature stabilization during crystal pulling results in a smooth increase of heating power.

Modified Stepanov/EFG growth using two-channel shape control is comparable with modified Czochralski technique and may be used for the growth of variable oxide crystals.

6. Automated Czochralski technique for semiconducting alloys

The peculiarities of the crystal growth of semiconducting alloys centre on the slow pulling rates which are necessary to avoid constitutional supercooling of the melt and an automatic control system must provide stable growth parameters during the long duration of growth [33]. To avoid constitutional supercooling the growth rate must not be higher than the critical growth rate determined by the Tiller criterion [34]. Automated Czochralski technique has been realized for the growth of both *Si*- and *Ge*-rich single crystals [35, 36].

Silicon-germanium alloys are advanced semiconducting materials containing the two main elemental semiconductors which form solid solutions across the whole composition range, i.e. they are complete miscible. $Si_{1-y}Ge_y$ is a promising material for application in electronics, optoelectronics and for basic research. Although $Si_{1-y}Ge_y$ is mostly used in the form of thin layers, bulk single crystals are required to study the fundamental properties of the alloys. Single crystals both of *Si*- and *Ge*-rich compositions are also interesting for X-ray, gamma ray and neutron optics. Especially *Si*-rich ($Si_{1-y}Ge_y$) gradient crystals based on the dependency of the lattice parameters resulting from the crystal composition can be used as monochromators for X-ray synchrotron radiation [37, 38]. In the case of *Ge*-rich ($Ge_{1-y}Si_y$) single crystals it was found that the addition of *Si* enhances slightly the mosaicity of the grown crystal. This allows to make monochromators for neutron beams and gamma rays well-tuned for special tasks [39].

The growth of *Si*- and *Ge*-rich crystals are two different processes because the segregation coefficient of *Ge* (minor component) in *Si* is less than 1 whilst the segregation coefficient of *Si* (minor component) in *Ge* is greater than 1. That is why the growth of *Si*- rich and *Ge*-rich single crystals will be analyzed separately.

6.1. Segregation coefficient of minor component less than unity

Czochralski apparatus with a resistance (graphite) heating element was used for the growth of $Si_{1-y}Ge_y$ single crystals with (111), (100), (110) or (211) orientation [35]. Quartz crucibles 74 mm and 95 mm in diameter were normally used for the growth of crystals up to 40 mm and up to 54 mm in diameter, respectively. *Si* seeds were used to grow $Si_{1-y}Ge_y$ single crystals from the melt with a starting *Ge* concentration of up to 7 at%. In the case of growth from the melt with an initial *Ge* concentration

of 7 at%-12 at% $Si_{0.97}Ge_{0.03}$ seeds were prepared from earlier-grown crystals. Final solidified fraction of charge $g = M_{cr}/M_0$, where M_{cr} - mass of crystal and M_0 - mass of charge *ab initio*, was about 0.9 in all experiments. Fig 15 shows a view of $Si_{1-y}Ge_y$ crystal growing from the melt with 7 at %Ge.

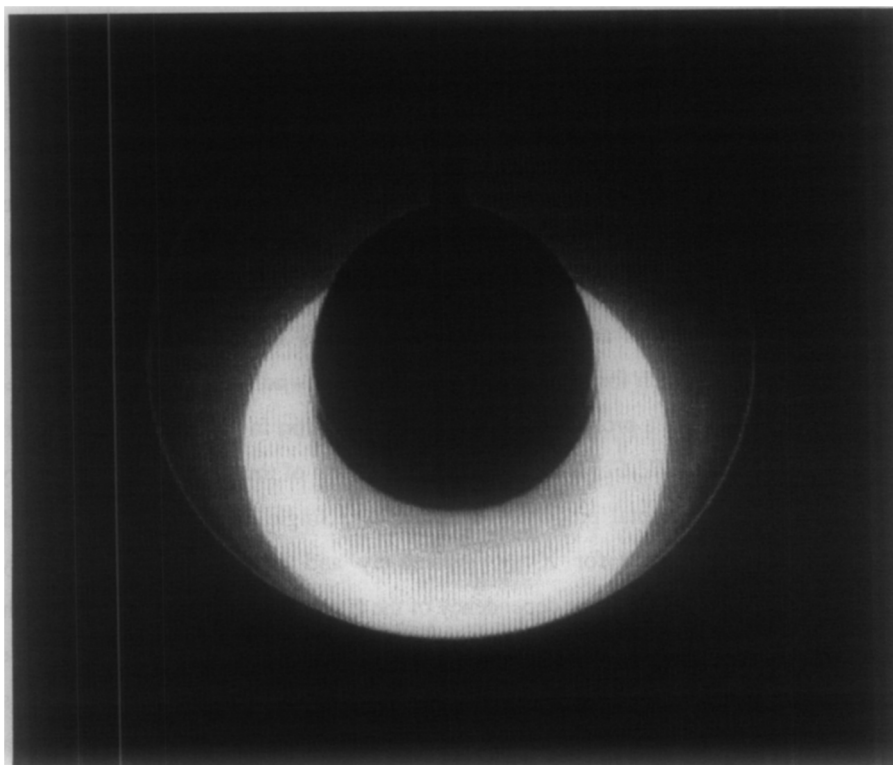


Fig. 15. View of $Si_{1-y}Ge_y$ crystal growing from the melt with 7 at %Ge

The computer controlled system used by the authors for the growth of $Si_{1-y}Ge_y$ single crystals is based on the application of a crystal weight sensor. The weight signal is used for automatic diameter control as the data source for feedback change of heating power. The electromagnetic weighing element has a sensitivity of approximately 10 mg. Controlling software provides also a feedforward control of process parameters. The user can define the change of the rates of pulling and rotation of crystal and crucible during the growth process according to certain mathematical functions of solidified fraction g . The solidified fraction g is calculated in real time for a preset crystal shape which is described by a smooth function of the crystal diameter for a growth length. Current values of crucible diameter (because of melt level decrease in a non-cylindrical crucible) and densities of solid and liquid phases are variable parameters in feedforward control.

Automatic diameter control is based on the use of a modified PID-controller relating to the deviation of the rate of weight change. The change of heating power resulting from PID-processing of the weight signal is limited to a certain value. As is known, the weight signal changes anomalously during the growth of semiconductors [21, 40]: sometimes, during decrease of crystal diameter, the deviation of the rate of weight change is positive, and at other times negative. In this case a simple PID-control leads to diameter oscillations [41]. To avoid such oscillations the “differentiated weight” mode is used for the stage of cylindrical growth and the technique of “modulating the heating power and cross-correlating it with weight signal” - for the conical section [42].

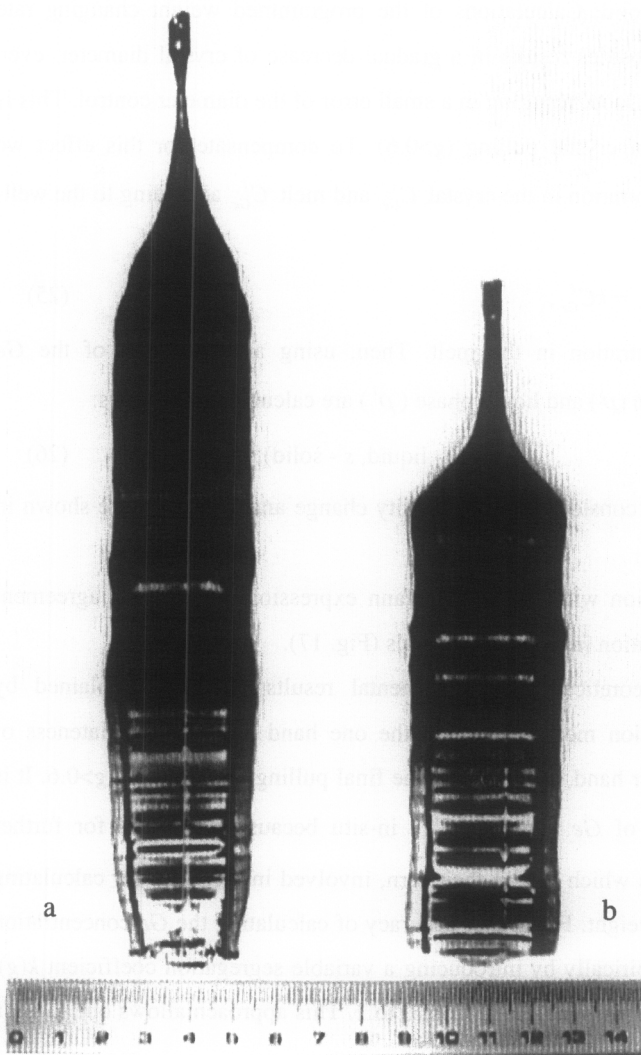


Fig. 16. $Si_{1-y}Ge_y$ single crystals grown by Czochralski method with 7 at% Ge ab initio in the melt under automatic diameter control (a) without and (b) with taking into account the change of solid and melt densities during the growth process.

For the growth of $Si_{1-y}Ge_y$ single crystals we use “second-derivative control” (also used for Czochralski growth of rare-earth molybdates) leading to the second derivative of weight being the main contribution to the signal for controlled heating power change. This contribution is large enough to limit the PID-calculated heating power change during most periods of control. Thereby, sufficient phase advance can be obtained and it provides a decrease of crystal diameter oscillations. By this means the heating power changes as a “sawtooth wave” curve which slowly decreases in average in the course of crystal pulling. The oscillating character of the heating power allows one to hold the meniscus in excited state and generate a “robust” weight signal.

In the case of $Si_{1-y}Ge_y$ crystal growth the segregation coefficient of Ge is less than 1 and, therefore, during the growth process the Ge content increases in the melt as well as in the crystal: it enhances the densities of liquid and solid. Calculations of the programmed weight changing rate presuming constant melt and crystal densities results in a gradual decrease of crystal diameter, even with optimal adjustment of the feedback loop, resulting in a small error of the diameter control. This is especially notable at the final stages of crystal pulling ($g > 0.6$). To compensate for this effect we estimate the current values of Ge concentration in the crystal C_{Ge}^s and melt C_{Ge}^l according to the well-known Scheil-Pfann expression:

$$C_{Ge}^l = C_{0,Ge}(1-g)^{k-1}, \text{ and } C_{Ge}^s = kC_{Ge}^l, \quad (25)$$

where $C_{0,Ge}$ is the initial Ge concentration in the melt. Then, using an estimation of the Ge concentration the densities of solid phase (ρ^s) and liquid phase (ρ^l) are calculated as follows:

$$\rho^i = \rho_{Si}^i + C_{Ge}^i(\rho_{Ge}^i - \rho_{Si}^i), \quad i = l, s \text{ (} l \text{ - liquid, } s \text{ - solid)}. \quad (26)$$

Crystals grown under the above considerations of density change and without it are shown in Fig. 16.

The estimates of Ge concentration with the Scheil-Pfann expression are in good agreement with experimental results for Ge distribution in as-grown crystals (Fig. 17).

Any disagreement between theoretical and experimental results could be explained by insufficient accuracy of the concentration measurement on the one hand and inappropriateness of Scheil-Pfann considerations on the other hand, especially at the final pulling stages, when $g > 0.6$. It is important to have a good evaluation of Ge content (C_{Ge}^i) in-situ because it is used for further calculation of solid and liquid densities which are, in their turn, involved in formulas for calculating the programmed crystal diameter and weight. For higher accuracy of calculating the Ge concentration in-situ we modified expression (1) empirically by introducing a variable segregation coefficient $k(g)$, which decreased linearly from 0.4 to 0.3 as g increased from 0 to 1. This approach allows one to get a better accordance with experimental results, Fig. 17.

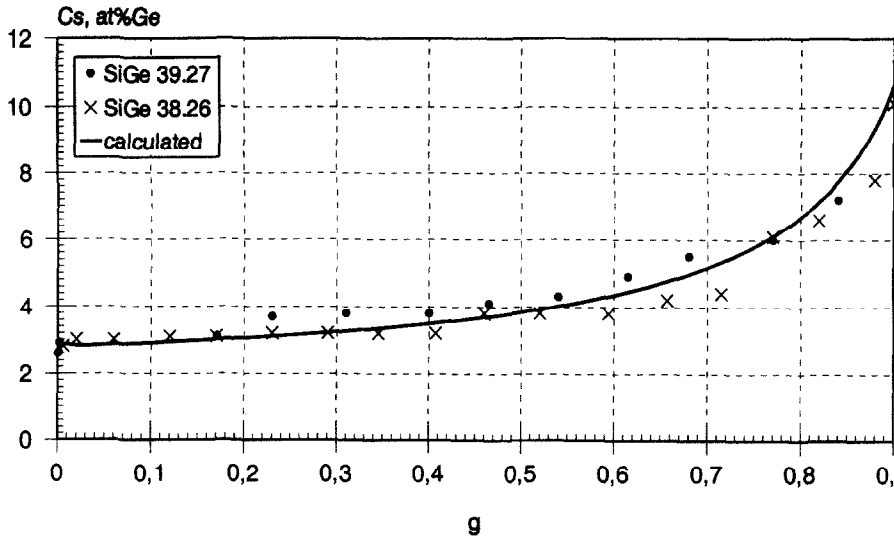


Fig. 17. Longitudinal Ge distribution (C_s) determined experimentally for two crystals shown in Fig. 15a (×) and Fig. 16b (·) and calculated by Scheil-Pfann expression with variable segregation coefficient $k(g)$. k is assumed to decrease linearly from 0.4 to 0.3 as the solidified fraction g increases from 0 to 1.

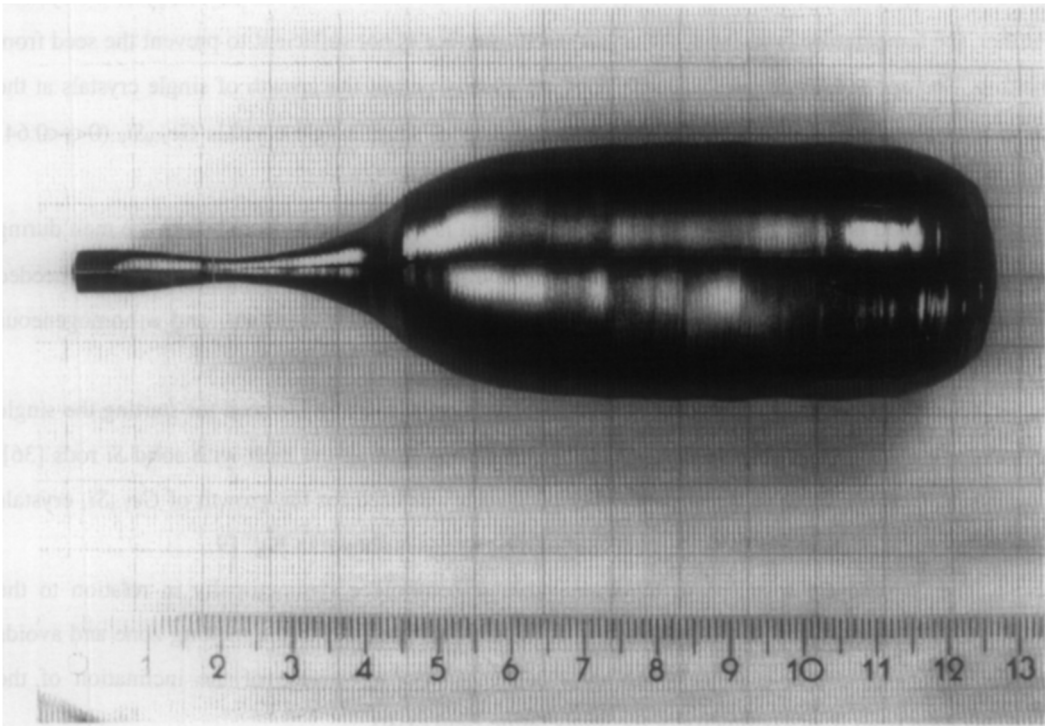


Fig. 18. $Si_{0.93}Ge_{0.07}$ single crystal grown with automatic diameter control.

The growth rate is a programmed parameter which should be optimized to get high productivity of the process and to avoid constitutional supercooling as was mentioned above. Growth rate is a sum of the rates of crystal pulling, crucible translation, decrease of melt level in a non-cylindrical crucible and change of meniscus height. During the Czochralski growth of $Si_{1-y}Ge_y$ single crystals the growth rate should be lowered with increase of solidified fraction. So we define in the controlling software the rates of crystal pulling and crucible translation as piece-wise linear functions of solidified fraction. In particular, in the case of growth from the melt with initial 7 at% *Ge* the melt composition changes from this value to nearly 20 at% *Ge* (when $g \approx 0.85$) and the optimal growth rate varies from 6 to 2 mm·h⁻¹, respectively. The crystal shown in Fig.18 was grown under this condition of growth rate optimization.

6.2. Segregation coefficient of minor component greater than unity

A different situation arises in the growth of $Ge_{1-y}Si_y$ crystals because the segregation coefficient of *Si* in *Ge* is greater than 1 and the *Si* concentration in the crystal decreases rapidly during growth. It is difficult to start the growth of highly concentrated $Ge_{1-y}Si_y$ single crystals. The use of *Ge* seeds is practically impossible because the melting temperature of *Ge* is the lowest in the binary *Si-Ge* system. Further, the temperature gradient at the crystal-melt interface is not sufficient to prevent the seed from melting. The application of pure *Si* seeds does not usually permit the growth of single crystals at the *Ge* side of the phase diagram [43], although the growth of small single crystals $Ge_{1-y}Si_y$ ($0 < y < 0.64$) started with pure *Si* seeds [44] has been reported.

A method is known [45] in which one component is charged continuously into the melt during the pulling process. The quantity of the feeding component increases smoothly until the needed concentration is reached. Then the composition of the melt is kept constant, and a homogeneous crystal of the solid solution is pulled.

Our approach in $Ge_{1-y}Si_y$ crystal growth is based on the use of a *Ge* seed for starting the single crystalline growth of the *Ge* crystal followed by continuous feeding the melt with solid *Si* rods [36]. Continuous feeding of the melt with a number of *Si* rods was used for the growth of $Ge_{1-y}Si_y$ crystals with a *Si* content of up to $y = 0.30$. A schematic of the process is shown in Fig. 19.

The *Si* rods are installed in the immovable screen-holder symmetrically in relation to the pulling axis. This provides an axial symmetry of the temperature field in the melting zone and avoids the probability of the crystal back-melting which could occur because of the inclination of the crystallization front if an asymmetry of the temperature field exists.

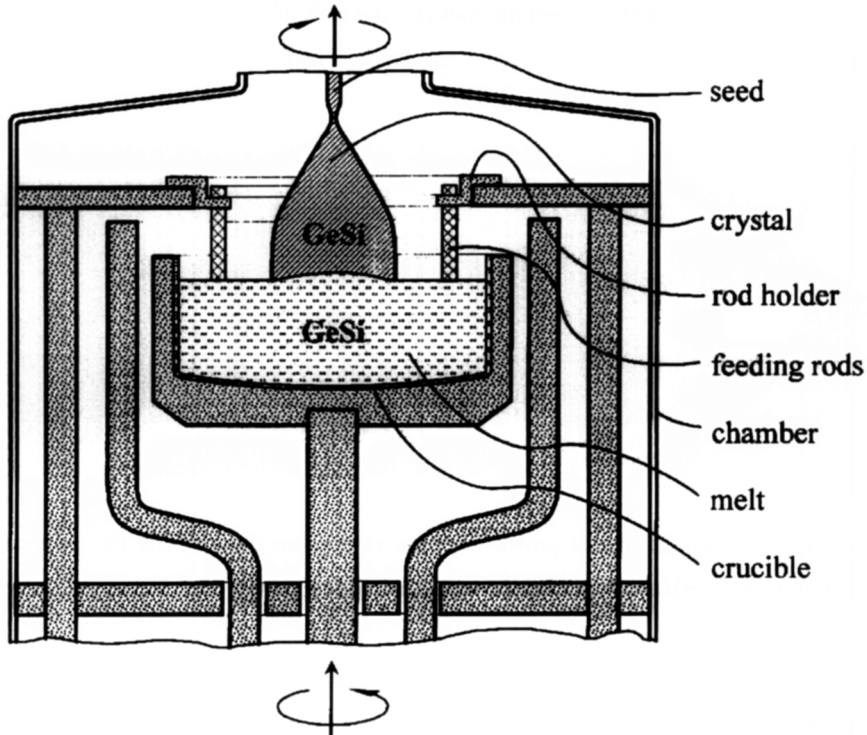


Fig. 19. Scheme of the growth of $Ge_{1-y}Si_y$ crystals with continuous feeding the Ge melt by solving of Si rods.

Crystal growth begins with a Ge seed which is dipped into a pure Ge melt. When a neck is formed and the crystal begins to expand the melt surface is contacted with the Si rods. The movement upwards of the crucible and its melt causes the Si rods to dissolve continuously in the Ge melt. The rate of crucible movement depends on the position of the rods in such a way that the silicon concentration gradient at the conical part of the crystal is maintained approximately constant. When the calculated concentration of Si in the crystal is achieved, equilibrium between the dissolved Si and the crystallizing Si component is attained. A $Ge_{0.98}Si_{0.02}$ single crystal grown by this technique is shown in Fig. 20. It is presumed that the Si rods begin to dissolve from the very beginning after their first contact with the surface of the Ge melt.

The dissolution process of Si in the Ge and the $GeSi$ melt was previously investigated experimentally [46]. According to these results the relative movement of the rod or the plate immersed into the melt does not influence the rate of dissolution. However in our experiments it was found that with melt overheating of about 30° in relation to the liquidus temperature (corresponding to the melt composition) the dissolution of the Si rods is complete 10–15 min. after immersing them into the melt,

without a relative movement between the rods and the melt. If such a movement between the rods and the melt exists the rate of silicon dissolution remains constant.

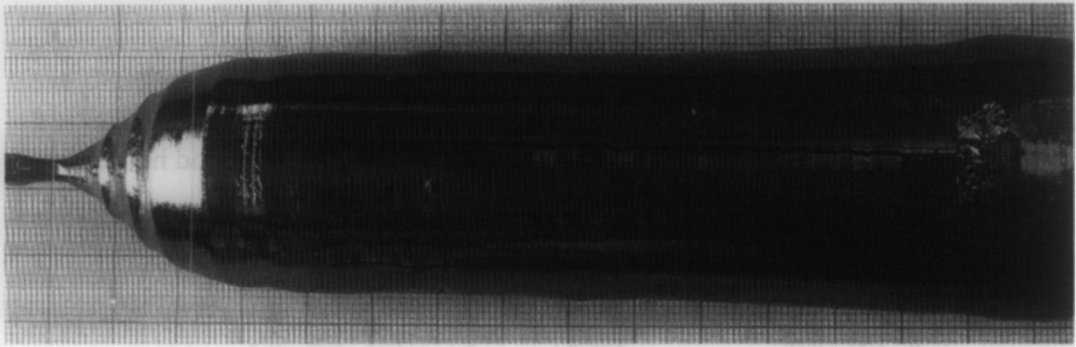


Fig. 20. $Ge_{1-y}Si_y$ crystal grown with the continuous feeding the Ge melt with Si rods. Si concentration is 2.0 ± 0.15 at% Si over the whole cylindrical part.

In the case of crystal pulling in the binary system $Ge-Si$, especially with high concentration of the second component, the expansion angle of the conical part must not be too large, because strong undercooling of the melt can lead, with high probability, to the destruction of single crystal growth. So it was necessary to expand the crystal from the neck at a small angle of the slope to the pulling axis.

The optimal conditions of $Ge-Si$ (with relatively large concentration of Si in Ge) crystal expansion ($\alpha < 20^\circ$) was found. This provides the maintenance of the single crystal growth. The temperature of crystallization increases with the increase of the Si concentration in a Ge melt in accordance with the phase diagram of the $Ge-Si$ system. Therefore, it is necessary to increase the heating power during crystal growth. It was found that a small decrease of heating power leads to the formation of a dendrite net on the melt surface and, as a result, to the transition into polycrystalline growth.

In the first experiments of $Ge_{1-y}Si_y$ crystal growth using weight control a PID regulator with limitation of the output signal was used [25]. The same regulator using second derivative control was applied to the processes of $Si_{1-y}Ge_y$ crystal growth. Direct application of this method of control to the automated pulling the $Ge_{1-y}Si_y$ crystals did not lead to positive results. To provide the automatic increase of heating power during the whole process of the $Ge_{1-y}Si_y$ crystal growth the application of a PID-regulator with asymmetrical control was used:

$$\Delta P := \begin{cases} k_+ \Delta P, & \text{if } \Delta P > 0 \\ k_- \Delta P, & \text{if } \Delta P < 0, \quad k_+, k_- \in (0, 1) \end{cases} \quad (27)$$

where k_+ and k_- are asymmetry coefficients of the positive and the negative semiwaves of the signal ΔP , respectively. The use of asymmetrical control allows one to avoid oscillations of the heating power resulting from the anomalous change of the weight signal and, as a result, to decrease the deviations of the lateral surface of the expanding crystal. In the process of pulling the crystal shown in Fig. 21 these coefficients had the following values: $k_+ = 1$, $k_- = 0.2$. Continuous increase of Si concentration of up to 14 at% in the conical part was achieved in this way. Single crystalline growth was observed up to a Si content $y = 0.1$.

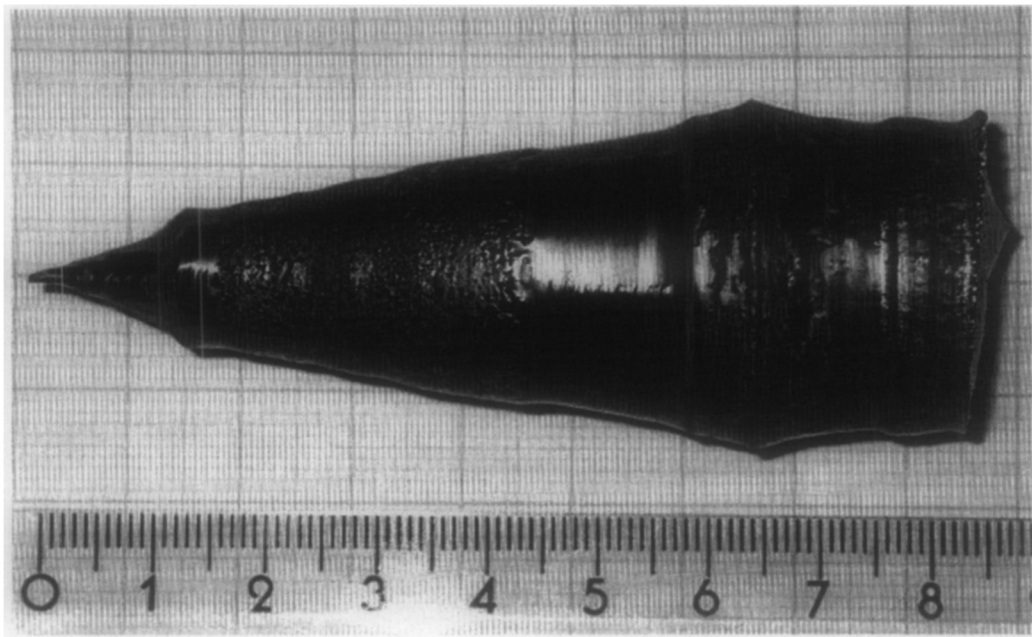


Fig. 21. $Ge_{1-y}Si_y$ crystal grown under asymmetrical control of the heating power.

7. Automated control of shaped crystal growth

7.1 Edge-defined film-fed growth (EFG)

The edge-defined film-fed growth (EFG) [47] technique was developed on the basis of the Stepanov [48] principle, namely that the shape or an element of shape is created in the liquid state, and then the shape or element is converted to the solid state by the use of appropriate crystallization conditions. In the EFG technique, crystals are grown from a melt film formed on the top of a

capillary die, Fig. 22. The melt rises to the crystallization front within the capillary channel. It is ideal for producing crystals with small square cross-section.

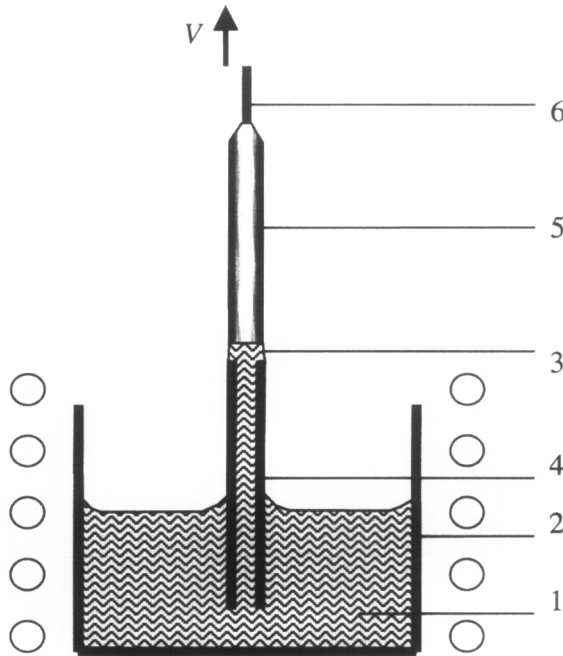


Fig. 22. The scheme of the EFG technique. 1 – melt; 2 – crucible; 3 – meniscus; 4 – die; 5 – crystal; 6 – seed.

By now the growth of sapphire crystal of various shapes is well developed by the efforts of different laboratories in the world. Currently, the most urgent problem in shaped crystal growth is to increase the crystal quality.

The most abundant defects in shaped crystals are gaseous and solid inclusions, as well as block boundaries. Their most probable origin is crystal supercooling (thermal or constitutional) and hence loss of the crystallization front stability [49-53]

In order to control the growth conditions at the crystallization front and prevent the formation of related defects an automated control system using a crystal weight sensor was applied to the process of shaped crystal growth. Automated computer systems provide *in situ* crystal quality control as well as crystal shape control, which permit an increase in the yield of high-quality crystals and the expansion of the areas of applications of sapphire crystals as constructional and optical material.

Direct application of automated control systems such as that developed for the Czochralski technique is unacceptable in the case of shaped crystal growth because of the anchoring of the meniscus to the edge of the die. This additional constraint for the growth of shaped crystal is the essential difference to the Czochralski technique.

The principles of automated control of shaped crystal growth with use of a crystal weighing technique have been developed [54] for the first time for all stages of the pulling process (seeding, crystal enlargement, stationary growth, *in situ* changing of the cross-section).

Regulation of the crystal cross-section has been achieved by controlling the deviation δM of the real mass M_r from the programmed mass M_p by variation of the heating power P . The real mass M_r is calculated from the measured weight signal W .

The meniscus height and the conditions at the melt-crystal interface, including supercooling and superheating, are closely related to the amplitude of oscillations of the deviation of the mass rate $\delta \dot{M}$. Together with analysis of mass deviation δM , its first $\delta \dot{M}$ and second $\delta \ddot{M}$ derivatives, the program also processes the amplitude of $\delta \dot{M}$ oscillations.

The measured parameter $\delta \dot{M}$ is a characteristic of the oscillatory mass rate deviation, always existing in any real growth process. The oscillation period is controlled by time characteristics of the actual process and a programmed regulator. The oscillation amplitude is controlled by thermal and response rates of a mechanical system.

The amplitude of the oscillations $\delta \dot{M}$ is related implicitly to the meniscus height and the position of the melt-crystal interface. One should choose the amplitude $\delta \dot{M}$ range and maintain the amplitude within this range during growth. A relatively small amplitude of $\delta \dot{M}$ indicates superheating of the melt-crystal zone and a rather large meniscus height. This may result in the appearance of facets on the lateral surface of the growing crystal with a decrease of cross-sectional area and, as a further sequence, a rupture of the meniscus. The upper boundary of the $\delta \dot{M}$ -amplitude is the most important parameter for automated growth of shaped crystals of high quality. A large $\delta \dot{M}$ -amplitude corresponds to supercooling in the melt-crystal zone, i.e. the meniscus height is correspondingly small. In this case a cellular structure can form on the melt-crystal interface, which leads to the formation of defects in the growing crystal. A further increase of the amplitude $\delta \dot{M}$ can lead to the partial freezing of the crystal to the die and to an undesirable change of crystal shape. The meniscus becomes so small that the crystallization front “sits down” on the working surface of the die.

7.1.1. Process of automated crystal seeding

Crystal seeding is an important stage of the growth process. The further stages of crystal growth depend on successful seeding. So the seeding process has found its own place in the general problem of automatization of shaped sapphire crystal growth.

There are two main versions of the seeding procedure [54]. In the first case the seed crystal partially melts, which results in a slow increase of the weight signal W . The value of the weight signal change is proportional to the area of seeding. The weight signal increase can be explained by the influence of the surface tension force on the weight signal. The surface tension force appears when the seed starts to melt, and this results in the melt meniscus formation between the seed and the shaper. Too extensive seed melting can result in the rupture of the meniscus and a sharp decrease of the weight signal. When meniscus rupture occurs the heating power is decreased automatically by a certain amount, and the seeding process has to be repeated. This “calculation-technological” cycle is repeated until the weight signal increases slowly or decreases (after its slow increase because of the meniscus formation) down to the value which is not less than that before the seeding cycle.

In the second case “cold” contact of the seed crystal and shaper occurs (without meniscus formation) and the weight signal W decreases sharply. After that the heating power will be increased step by step until meniscus formation starts.

The process of the automatic crystal seeding is tuned by a specific set of software parameters to get a stable “calculation-technological” iteration process. The most important parameters which influence the stability of the crystal seeding process are as follows:

- maximum rates of seed crystal lowering and lifting;
- minimum time interval for the evaluation of the weight data change;
- minimum time interval for melt exposure for a specific value of heating power;
- minimum step in the heating power change.

Crystal pulling starts when the controlling computer has “understood” that crystal seeding has been successfully achieved. Crystal enlargement proceeds if the weight signal W increases gradually with a sufficiently small $\delta\dot{M}$ -amplitude. The absence of a gradual increase of the weight signal or too a large $\delta\dot{M}$ -amplitude during the first moments of crystal pulling indicate supercooling in the melt-crystal zone. In this case the computer will automatically increase the heating power until the weight signal starts to grow gradually with a sufficiently small $\delta\dot{M}$ -amplitude and then the process of crystal expansion will begin.

7.1.2. Calculation of the programmed mass change for the tube enlargement

Consideration of the problem below is based on the case of the movement of the crucible according to the melt level change. In this case the distance between the working surface of die and the melt level should be constant.

Enlargement of the crystal tube up to the die size was found to be the critical factor for high-quality crystal growth.

Calculation of the program mass for various profiles can be determined by integrating the preset crystal shape. For single point seeding (Fig. 23) the shape of growing crystal is defined by the function of the angle $\alpha(z)$ of the slope of the crystal unwrapping curve $\tilde{l}(z)$ to crystal pulling axis Z.

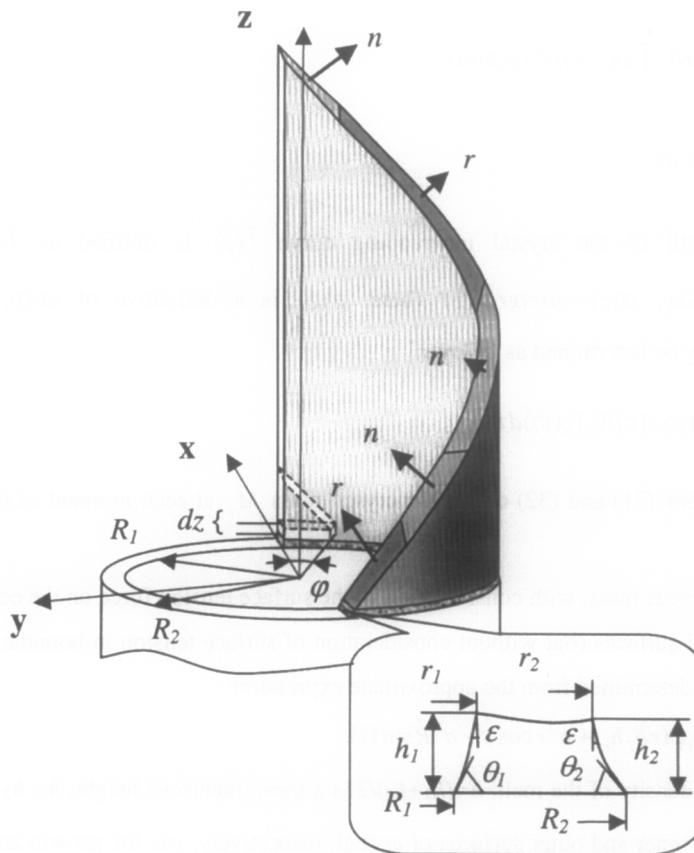


Fig. 23. Tube growth scheme for calculation of the program mass at one point seeding.

The mass M_d that is weighed with the weight sensor is the sum of the mass M_s of the solidified fraction of the melt and the mass M_l of the meniscus (with consideration of the surface tension force) [21]:

$$M_d = M_s + M_l. \quad (28)$$

The crystal mass change dM_s during a small time interval dt is determined as follows:

$$dM_s = \rho_s r \delta_T \varphi(z) V_c(z) dt, \quad (29)$$

where ρ_s is crystal density, $r=r_1+r_2$ is a mean tube radius, r_1 and r_2 are inner and outer crystal radii, respectively, $\varphi(z)$ is the angular coordinate of the boundary segment of crystal enlargement in the cylindrical system of coordinates (r, φ, z) and $V_c(z)$ is the crystallization rate (generally, it is not constant). Using Eq. (29) one can obtain the rate \dot{M}_s of crystal mass change:

$$\dot{M}_s = \rho_s r \delta_T \varphi(z) V_c(z). \quad (30)$$

The mass M_s of growing crystal may be got by integrating Eq. (30):

$$M_s = \rho_s r \delta_T \int_{t_0}^t \varphi(z(\tau)) V_c(z(\tau)) d\tau, \quad (31)$$

where $z(t) = \int_{t_0}^t V_c d\tau$.

The length of the crystal unwrapping curve $\tilde{l}(z)$ is defined as $\tilde{l}(z) = r\varphi(z)$. Then, $tg\alpha(z) = d\tilde{l}(z)/dz$, $\alpha(z) = arctgr\varphi'(z)$ (here $\varphi'(z)$ is a derivative of $\varphi(z)$), and an angular coordinate φ may be determined as follows:

$$\varphi = \frac{1}{r} \int_{t_0}^t tg\alpha(z(\tau)) V_c(z(\tau)) d\tau, \quad (32)$$

Expressions (31) and (32) define the crystal mass M_s at each moment of time for the preset shape of crystal.

The meniscus mass, with consideration of the surface tension force on the edges of the die and the lateral crystal surfaces (but without consideration of surface tension in boundary segments of the cross-section) is determined from the approximate expression:

$$M_l = 2\rho_l \varphi (r\delta_T h_m + a^2 r \cos \varepsilon - a^2 R \sin \Theta), \quad (33)$$

where ρ_l is the density of the melt, $h=(h_1+h_2)/2$ is a mean meniscus height, h_1, h_2 are the heights of meniscus on the inner and outer surfaces of crystal, respectively, ε is the growth angle, $R=(R_1+R_2)/2$ is a mean radius of the die, R_1, R_2 are the radii of inner and outer edges of the die respectively and $\Theta=(\Theta_1+\Theta_2)/2$ is a mean angle between meniscus and working surface of the die, with Θ_1, Θ_2 the

contact angles between meniscus and the working surface of the shaper at inner and outer shaper edges, respectively.

The shape of the melt-crystal interface, values of the meniscus heights h_1 , h_2 , and contact angles θ_1 , θ_2 can be determined from the coupled numerical solution of the capillary and Stefan problems. These problems are not considered for arbitrary profiles in our controlling software. Instead of the exact values of the above parameters approximate estimations are used.

The expressions (31)–(33) define the programmed mass change for a preset crystal shape.

For sapphire tubes of large diameter grown along the C -axis, the most remarkable occurrence at this stage was the appearance of inclined facets at the end surface [55]. This surface was defined by the sequential appearance of positive rhombohedral planes r ($\{10\bar{1}1\}$, $\{0\bar{1}11\}$, $\{\bar{1}101\}$) and the dipyramidal planes n ($\{4\bar{2}\bar{2}3\}$, $\{2\bar{4}23\}$, $\{\bar{2}\bar{2}43\}$, $\{\bar{4}223\}$, $\{\bar{2}4\bar{2}3\}$, $\{2\bar{2}\bar{4}3\}$), Fig. 24. During the enlargement of the tube, up to the die size, the transition from one plane to another may be of three types: $n \rightarrow r$, $r \rightarrow n$ and $n \rightarrow n$. The angle between the perpendicular to r -planes and the C -axis is 57.6° and the angle between the perpendicular to n -planes and the C -axis is 61.2° [56].

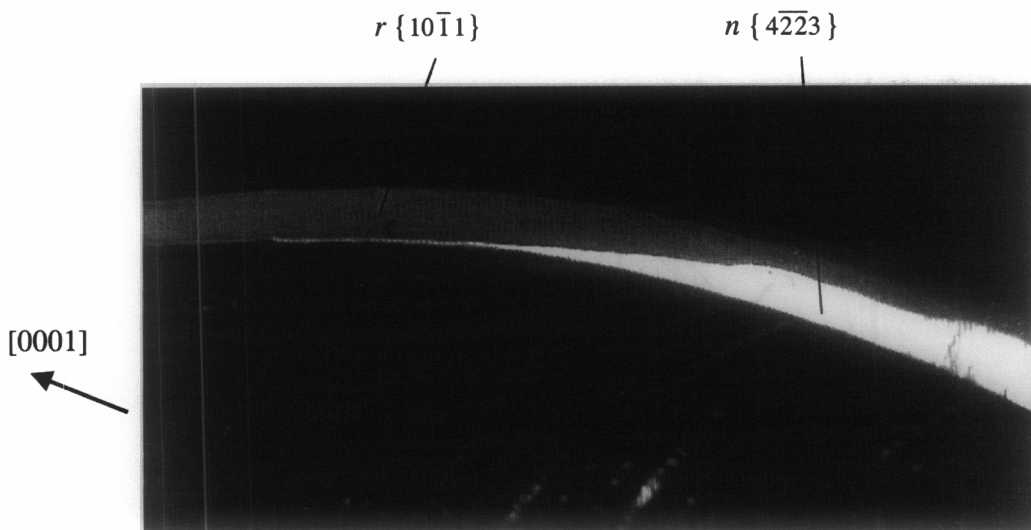


Fig. 24. Faceting of sapphire tubular crystal of 85 mm in diameter: the r - and n -planes at the end surface.

To optimize the enlargement of a sapphire tube, one should change the angle on the unwrapping curve according to r - and n -planes (Fig. 23).

Let $\{\varphi_i\}$ be a sequence of azimuthal angles between centres of rhombohedral and dipyramidal planes having the declination angles $\{\alpha_i\}$ to the vertical. Obviously, if one maintains $\{\alpha_i\}$, then the current crystal length l is defined by the sequence $\{\varphi_i\}$. In particular, if one assumes a discrete transition from one plane to another, neglecting smooth plane transition, then the current length l_c is defined by:

$$l_c = r \sum_{i=1}^k \text{ctg} \alpha_i (\varphi_{i+1} - \varphi_i) + r \text{ctg} \alpha_{k+1} (\varphi - \varphi_{k+1}), \quad \varphi > \varphi_{k+1}, \tag{34}$$

where k is the number of already grown plane, $k+1$ is the number of growing plane.

The current length is known since it is integral of the pulling velocity. Therefore, Eq. 34 can be used to find the current angular coordinate of the profile φ depending on the sequence $\{\alpha_i\}$ to calculate the programmed mass.

The length of enlargement depends on the tube radius $r=r_1+r_2$ and the averaged declination angle α , given by the equation $l=\pi/r\text{tg}\alpha$. Obviously, the value of α that needs to be maintained in the course of the enlargement stage is in the range of 28.8° ($90^\circ-61.2^\circ$) to 32.4° ($90^\circ-57.6^\circ$). In this case, the optimum length is in the range $l=(4.96-5.72)r$.

In practice, the enlargement from two opposite die points (with two point seeding) is of interest, Fig. 25.

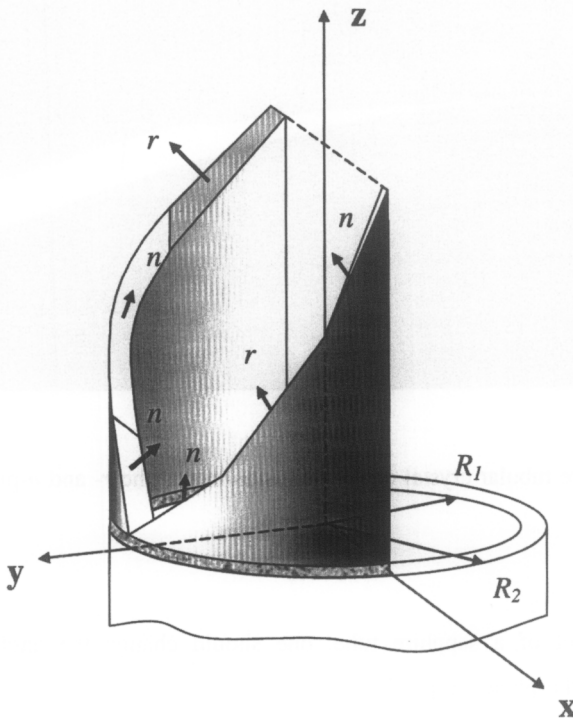


Fig. 25. Tube growth scheme for calculation of the program mass at two point seeding.

For a pair of growing profiles, two current azimuthal angles φ_1 and φ_2 are calculated to depend on different sequences $\{\varphi_{ij}\}$ and $\{\alpha_{ij}\}$ ($j=1,2$) of azimuthal and vertical angles of rhombohedral and dipyramidal planes. For different sequences $\{\alpha_{i,1}\}$ and $\{\alpha_{i,2}\}$, defined by seed orientations, the encounter point is shifted relative to the horizontal symmetry axis at the seeding points, which is perpendicular to the line connecting them. The shift of the seeding point f relative to the symmetry axis is written as:

$$f = r \sin|(\varphi_1 - \varphi_2) / 2|. \quad (35)$$

where φ_1 and φ_2 are taken at the junction of two profiles.

7.1.3. Calculation of the programmed mass change for the plate enlargement

The grown profile for the plate is defined by the angle $\alpha(z)$ of the plate lateral profile to the crystal pulling axis [57], Fig. 26. The mass M_d measured by the weight sensor is composed of crystallized melt and meniscus masses M_s and M_l .

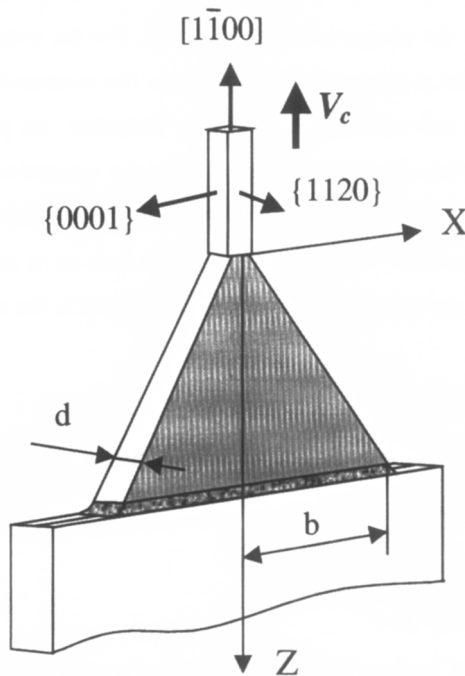


Fig. 26. Schematic illustration of plate growth by EFG technique.

The crystal mass rate \dot{M}_s is given by:

$$\dot{M}_s = b(z)d\rho_s V_c(z), \quad (36)$$

where b and d are the plate width and thickness, respectively, ρ_s is the crystal density, and V_c is the crystallization rate. The growing crystal mass M_s is found by integrating Eq. (36):

$$M_s \approx bdh_m \rho_l, \quad (37)$$

where ρ_l is the melt density and h_m is the meniscus height. The rate of mass increase of the growing crystal is approximately written as:

$$\dot{M}_l = 2dh_m \rho_l V_c(z) \operatorname{tg} \alpha(z). \quad (38)$$

The crystallization front shape and meniscus height can be found by simultaneous solution of the capillary problem and the Stefan thermal problem. In the control system this problem is not solved and estimations are used instead of exact values.

7.1.4. In situ correction of the programmed mass change

Since the meniscus parameters can not be calculated exactly during the growth process, especially for the complicated cross-sections of crystals and multi-crystal processes, Eqs. (31)–(33), (36), (37) can not exactly describe the programmed mass change. For the compensation of error of this calculation one parameter of the meniscus is corrected from the measured weight signal, other “doubtful” parameters of meniscus and crystal being constant. Therefore one parameter involved in Eqs. (31)–(33), (36), (37) is adjusted so as to compensate for the estimation errors of the other parameters. For this selected parameter an equation must be solved. There is an expression similar to Eq. (28) in the left side of the equation and with the measured mass data on its right side.

In the case of sapphire tube growth the tube thickness is selected as the tuning parameter, and it is determined from the equation:

$$\dot{M}_s(\delta_r^r(t)) + \dot{M}_l(\delta_r^r(t)) = \dot{M}_r(t), \quad (39)$$

where $\dot{M}_r(t)$ is the measured real mass rate data depending on time, and $\delta_r^r(t)$ is the “real” tube thickness that should be calculated from Eq. (39). Using Eq. (39) we can find the tube thickness:

$$\delta_r^r(t) = \frac{\frac{1}{2}\dot{M}_r(t) - \rho_l a^2 (\cos \varepsilon - \frac{R}{r} \sin \Theta) V_c \operatorname{tg} \alpha}{\rho_s r \varphi V_c + \rho_l h V_c \operatorname{tg} \alpha}. \quad (40)$$

In the case of enlargement of a plate, the plate thickness d is used as a free variable. During the process, the equation

$$\dot{M}_s(d^r(t)) + \dot{M}_l(d^r(t)) = \dot{M}_d^r(t), \quad (41)$$

(where $\dot{M}_d^r(t)$ is the measured real mass rate data depending on time) is used to find the “real” profile thickness $d^r(t)$ of the plate:

$$d^r(t) = \frac{\dot{M}_d^r(t)}{\rho_s b V_c + 2 \rho_l h_m V_c t g \alpha}. \quad (42)$$

Note that the tube and plate thickness as calculated from Eqs. (40), (42) can strongly differ from the real thickness of the tube or plate and depends on the accuracy of values of other “weakly-known” parameters of the crystal and meniscus that are involved in Eqs. (40), (42).

At the first moments of crystal expansion the control parameters of the software provide a “mild” automated control based mainly on manual regulation. At this stage it is necessary to observe the state of the melting zone, i.e. to analyze the excessive overheating or overcooling of the crystal, and to observe the behaviour of the deviation $\delta \dot{M}$ and calculated thickness $\delta_r^r(t)$ for tube and $d^r(t)$ for plate growth. Then the user makes corrections of the programmed mass rate \dot{M} by adjustment the programmed thickness d or δ_r and fully entrusts the crystal regulation to the computer.

The use of crucible translation is also necessary for shape and quality control. The rate of crucible translation is calculated according to the change of melt level during the crystal growth process. It is important to maintain a constant distance between the working edges of the shaper and the level of the melt in the crucible to keep a sufficiently constant thermal gradient in the shaper and constant hydrostatic pressure in the meniscus. Additional changes of the crucible translation rate can be used for control of the crystal shape and quality.

7.1.5. Steady state growth

At the steady state growth stage the programmed rate \dot{M} of mass increase is constant and controlled by the cross-section of the crystal. As was shown above, the grower can correct \dot{M} to improve growth conditions by changing the programmed tube (δ_r) or plate (d) thickness or another geometrical parameter (in the case of an arbitrary shape). One can observe and analyze the behaviour of the deviation $\delta \dot{M}$ on the computer display without visual inspection of the state of the molten zone.

In the case of plate growth the required plate thickness is estimated by Eq. (42) simplified to:

$$d^r(t) = \frac{\dot{M}_r(t)}{\rho_s b V_c} \quad (43)$$

for the steady state growth stage.

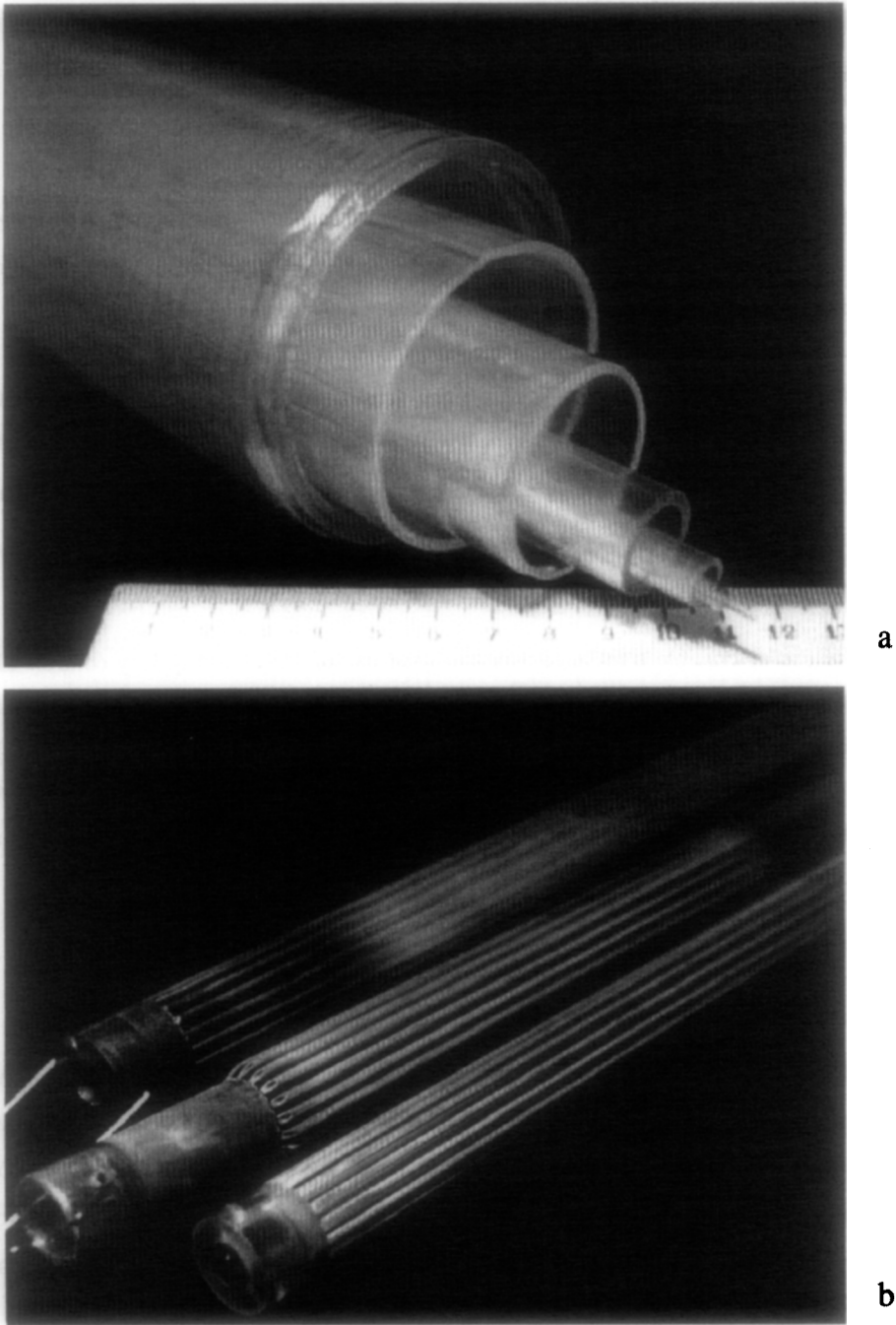


Fig. 27. Sapphire crystals grown by Stepanov/EFG technique with automated control: (a) tubes with diameter up to 85 mm; (b) rods 3.0 mm in diameter and tubes 3.5 mm in outer diameter grown by multi-run pulling process.

An optimum seed orientation is extremely important to produce a large-scale high quality sapphire plate. Growth experiments with plates of various orientations have shown that plate growth perpendicular to the C axis is the most preferred to prevent small-angle grain boundary formation. The plates are pulled in the direction of a hexagonal prism m $[1\bar{1}00]$, the plate plane coincides with a plane a $\{11\bar{2}0\}$, and the basis plane C $\{0001\}$ is a plate lateral face (Fig. 26). Due to the singular minimum of the specific free surface energy, the outer crystal surface has an energetically favourable orientation as the angle between meniscus and face (or the meniscus height) is varied, i.e. a mirror face is formed at the outer surface of growing crystal [58].

If the lateral faces of the plate comprise the singular face $\{0001\}$ this significantly increases the temperature range during crystal growth due to the high stability of the face adhered to the die edges. The steady state growth shift toward higher temperatures elevates the meniscus (increases the angle between meniscus and face) with no substantial change in the plate cross-section. The expanded temperature range is extremely important when growing several plates in multi-run growth processes and wide plates with a non-uniform thermal field in the die or dies.

Along with power control, crucible displacement is also effectively controlled. First, the rate of crucible translation is calculated according to the change of the melt level during the crystal growth process. It is important to maintain a constant distance between the working edges of the die and the level of the melt in the crucible. This distance should maintain a sufficiently constant thermal gradient in the die and constant hydrostatic pressure in the meniscus to improve the crystal quality. Second, a fixed displacement of the crucible in combination with weight control is used for the control of the crystal shape and quality.

The growth experiments were carried out in an 8 kHz induction heated graphite susceptor/molybdenum crucible set up. The raw material was crushed Verneuil boules. An argon atmosphere under a pressure of 1.1–1.2 atm was used as ambient.

Sapphire tubes with diameter up to 85 mm (Fig. 27a) [59] and ribbons of 120 mm width for optical applications [60] have been grown using the automated control system. A multi-run pulling process with *in situ* quality control provides an increase in growth productivity. Sapphire crystals in shape of the rods and tubes with up to 50 crystals per pulling process were grown by a multi-run system [54], Fig. 27b.

7.2. Non-Capillary Shaping (NCS) technique

The main feature of the NCS technique is the delivery of the melt to the growth interface through a non-capillary channel via a wettable die [61], (Fig. 28). The melt column has negative

pressure as in the EFG method. The word “non-capillary” indicates here that the diameter of the channel is greater than the value of the capillary constant.

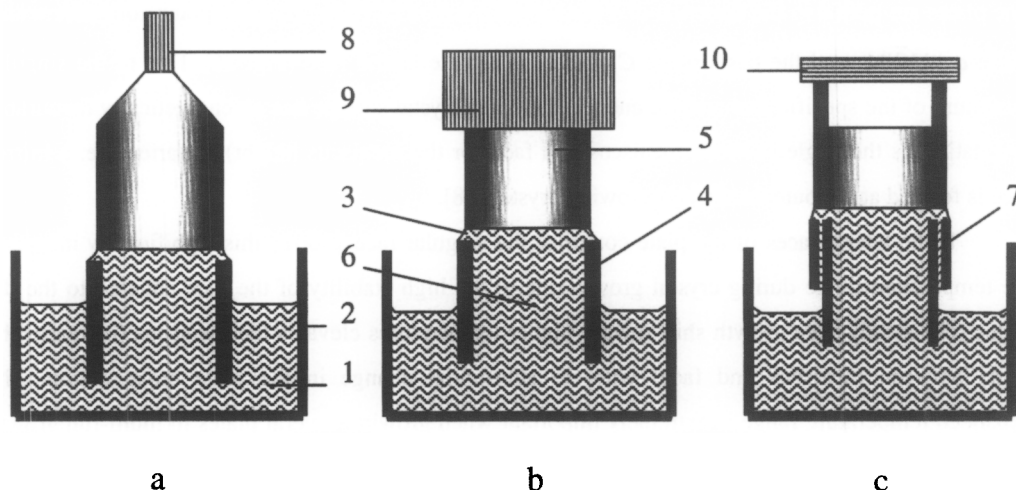


Fig. 28. Schemes of various variants of bulk crystal growth by the NCS technique using different seed shapes: a – with the use of a point seed; b – with the use of a bulk seed; c – with the use of the pressure difference in a growth chamber and inside a closed volume under a seeding plate. 1 – melt; 2 – crucible; 3 – meniscus; 4 – die; 5 – crystal; 6 non-capillary channel; 7 – capillary channel; 8 – point seed; 9 – bulk seed; 10 – plate seed.

The NCS method, as distinguished from the technique based on the traditional capillary feed, ensures the absence of micro-voids and gaseous and solid inclusions which are formed in the regions with the minimal components of a melt velocity below the crystallization front. The dominant flow always moves from the centre to the periphery irrespective of the crystal cross-section, thus enabling the growth of large sapphire crystals free of bulk inhomogeneities. The formation of the optimal interface surface and the hydrodynamic flows of the melt under the crystallization front are determined by the shape of the top surface of the die, by the velocity of growth and by the size of the non-capillary channel.

The NCS technique can include combinations of the Stepanov/EFG technique and the non capillary shaping of a rod. Automated weight control in these cases is similar to the control in corresponding Stepanov/EFG and Czochralski techniques with some differences. In these type of techniques it is necessary to maintain the geometrical parameters of the growing crystal more exactly than in the Czochralski technique because the geometry of the crystal is connected with the geometry of the die, as a rule, by a small enough liquid meniscus. Therefore, additionally to the ordinary PID-

procedure for calculation of the heating power change the $\delta\dot{M}$ -amplitude is analyzed. According to the value of this amplitude a geometrical parameter of the cross-section of the growing crystal is corrected. Thus, a second closed loop of control is used in the non-capillary shaping technique.

The use of automated control in the NCS method is also important for all stages of crystal pulling (seeding, cross-section changing, stationary growth).

For the growth of bulk crystals, different kinds of the initial growth stage and the subsequent feeding via a non-capillary channel can be used: with a small seed (Fig. 28a), bulk seed (Fig. 28b), and ring-shaped capillary channel with the use of a pressure difference in a growth chamber and inside a closed volume under a seeding plate (Fig. 28c) [61–63]. Seed rotation can be used simultaneously with its advance at the stages of seeding, transient growth and steady-state growth. In all these cases the shape of the bulk crystal is determined by the catching at the outer edge of the die.

Using a small seed, crystal seeding and further enlargement up to the edges of the die is similar to the Czochralski method. Algorithm [17] for enlargement of the crystal from the seed to cylindrical portions is similar to the Czochralski method. The optimal functional dependence of the angle of the tangent to a vertical is described as $\alpha(r) = \sin^2 \pi (r - r_0) / (r_0 - r_f)$, where r_0 , r and r_f are the respective initial, current and final radii.

In the case of seeding on a bulk seed (Fig. 28b) or a plate (Fig. 28c) the condition of the seed at the moment of contact with the die, formation of a melt meniscus over all of the perimeter of the die and the thermal conditions at the crystallization front should be controlled.

It is important to make automated transition from the growth of tube to the growth of rod. For this purpose the shape of the transition portion of the crystal is approximately described by a linear piece-wise function according to the results of manual crystal growth processes, (Fig. 29). Using this linear piece-wise description of this shape, the expression for the programmed weight signal is constructed which is then used for the PID-procedure and for a second closed-loop control.

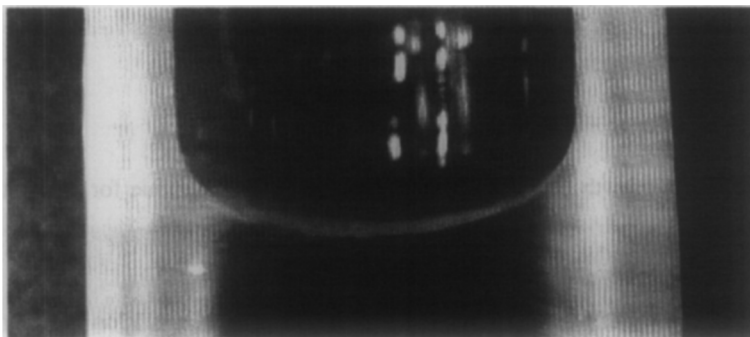


Fig. 29. Transitional part of sapphire crystal of 34 mm in diameter grown by the NCS technique.

The expression for the programmed mass is:

$$M = \pi\rho_s(r_2^2 - r_1^2)l_1 + \pi\rho_s(r_2^2 \int Vdt - \int r^2(l)Vdt) - H_d\rho_L((r_2 + \delta_2)^2 - (r(l) - \delta_1)^2) + \pi\rho_L(r_2 - r(l))^2 h_m + 2\pi\rho_L(a^2 r_m \cos \varepsilon - a^2 r_d \sin \Theta_m), \quad (44)$$

where r_1 and r_2 are inner and outer crystal radii of a tube; l_1 is the length of a tubular part of a crystal to the beginning of the transition portions; ρ_s and ρ_L are crystal and melt density, respectively; V is the crystal pulling rate; H_d is the distance from the level of the melt surface up to the working edges of the die (in the considered case $H_d < 0$); δ_1 and δ_2 are the respective sizes of projections of internal and external parts of the meniscus on a horizontal plane of the die (Fig. 30); $h_m = (h_1 + h_2)/2$ is the mean meniscus height; $r_m = (r(l) + r_2)/2$ is the mean meniscus radius; ε is the growth angle; $\Theta_m = (\Theta_1 + \Theta_2)/2$ is the mean angle between meniscus and working surface of the die.

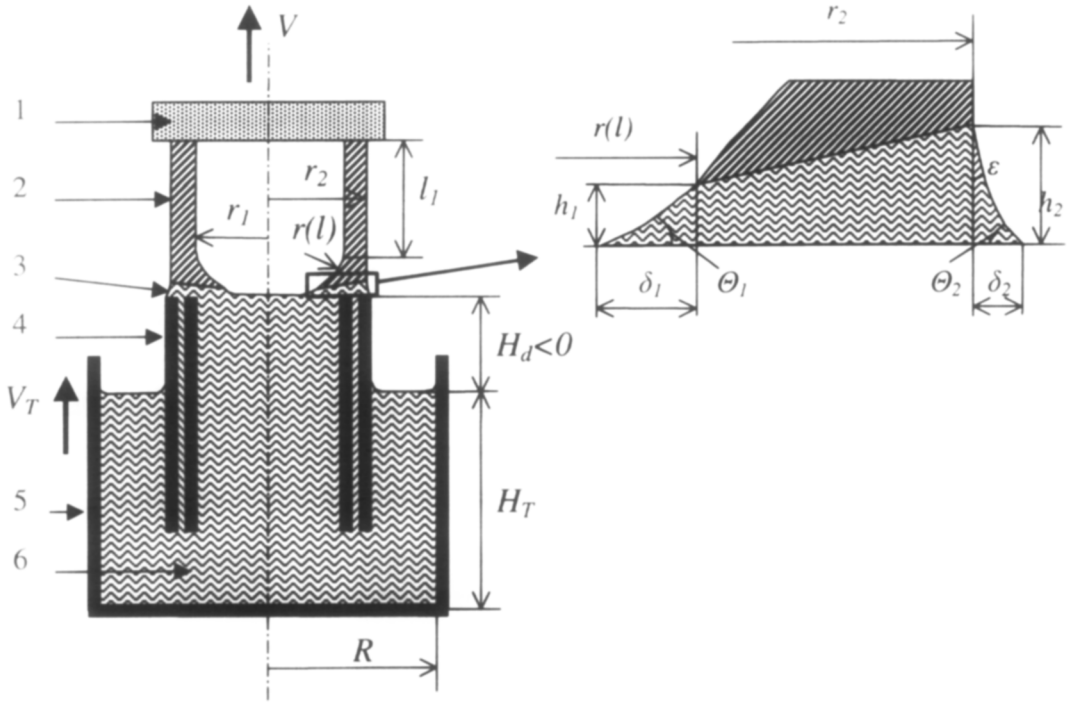


Fig. 30. Scheme of growth of transitional part by the NCS technique for calculation of the program mass.

In parallel with control of power, control of the rate of crucible translation is effectively used for maintenance of a constant of distance from working surface of the die and melt level in the crucible.

The rate of crucible translation is calculated according to the shape of the growing crystal and its pulling rate.

$$V_r = \frac{\rho_s(r_2^2 - r^2(l))}{\rho_L(R^2 - \frac{S_d}{\pi})} V, \tag{45}$$

where R is the radius of the crucible; S_d is the area of the die cross-section.

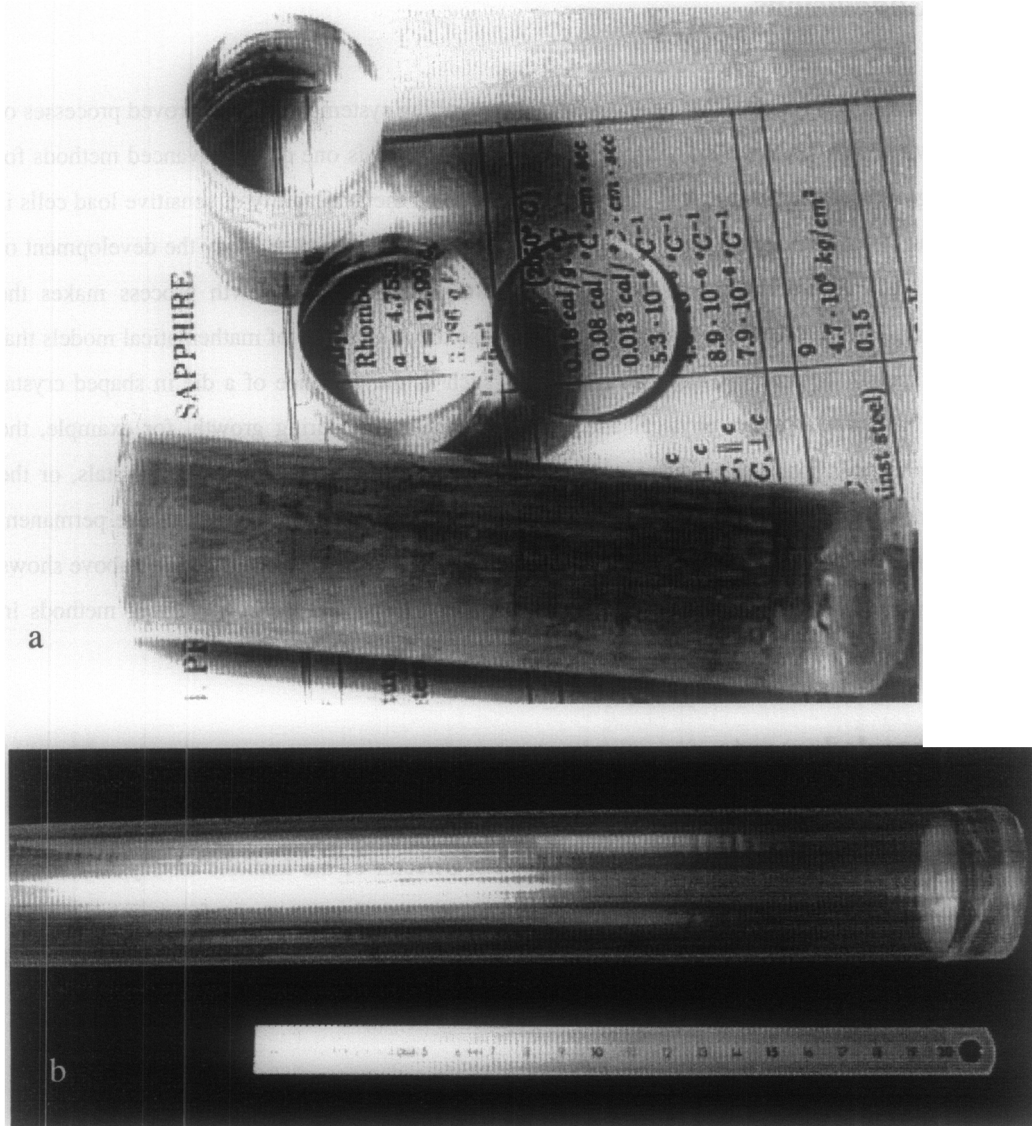


Fig. 31. Sapphire crystals grown by the NCS technique: (a) rods of 35 mm in diameter; (b) crucible of 40 mm in outer diameter.

The NCS method with use of automated control has been successfully realized for growth of high-quality sapphire crystals of any predetermined cross-section, constant along the crystal length (rods of various cross-sections for optical applications, thick ribbons and tubes with large wall thickness), and crystals with discretely changing cross-section configuration (domes, boats, crucibles), Fig. 31.

8. Conclusions

It has been shown above that high developed controlling systems lead to improved processes of crystal growth. The use of weight control of the growing crystal is one of the advanced methods for automated growth of a wide range of materials. Nevertheless the availability of sensitive load cells is necessary but not sufficient for the realization of automated crystal growth. Only the development of controlling software for the processing of crystal weight during the growth process makes the controlling system complete. Such software assumes also the availability of mathematical models that include the specific features of the growth methods such as the presence of a die in shaped crystal growth and take into account physical and chemical phenomena during growth, for example, the crystallographic anisotropy that causes a non-circular cross-section of the growing crystals, or the change of melt composition during the growth of semiconducting alloys that causes the permanent change of the crystal and melt density. The examples of the growth processes described above shows ways of improvement of automated control systems and the importance of weighting methods in crystal growth.

Acknowledgments

Authors wish to acknowledge Prof W. Schröder, Director of the Institute of Crystal Growth, Berlin for his support in the realization of some ideas on the development of automated control systems. We also wish to thank Dr. G.A. Satunkin for useful discussions during the preparations of this review and Prof. J.B. Mullin for his valuable advice.

References

1. D.T.J. Hurle, *J. Crystal Growth*, v. 42, 1977, p. 473.
2. D.T.J. Hurle, B. Cockayne, in: *Handbook of Crystal Growth*, Ed. D.T.J. Hurle (Elsevier, Amsterdam, 1994), chapter 3, p. 99.
3. T.G. Digges, R.H. Hopkins, R.G. Seidensticker, *J. Crystal Growth*, v.29, 1975, p. 326.
4. U. Gross, R. Kersten, *J. Crystal Growth*, v. 15, 1972, p. 85.
5. R.E. Lorenzini, F.S. Nuff, D.J. Blair, *Solid State Tech.*, Feb. 1974, p. 33.
6. H.D. Prueett, H.Y. Lien, *J. Electrochem. Soc.*, v. 121, 1974, p. 822.
7. H.J.A. VanDijk, C.M. G.Jochern, G.J. Scholl, P. VanderWerf, *J. Crystal Growth*, v. 21, 1974, p. 310.
8. D.F. O’Kane, T.W. Kwap, L. Gulitz, A.L. Bednowitz, *J. Crystal Growth*, v. 14/14, 1978, C24.
9. V.I. Goriletkii, B.V. Grinyov, B.G. Zaslavskii, N.N. Smirnov, V.S. Suzdal “Crystal growth (alkali halides).” (*Acta*, Kharkov, 2002, 536 p.), (in Russian).
10. W. Bardsley, G.W. Green, C.H. Holliday, D.T.J. Hurle, *J. Crystal Growth*, v. 16, 1972, p. 277.
11. R.C. Reinert, M.A. Yatsko, *J. Crystal Growth*, v. 21, 1974, p. 283.
12. G. Zydzik, *Mat. Res. Bull.*, v. 10, 1975, p. 9.
13. A.J. Valentino, C.D. Brandle, *J. Crystal Growth*, v. 26, 1974, p. 1.
14. W. Bardsley, B. Cockayne, G.W. Green, D.T.J. Hurle, G.C. Joyce, J.M. Roslington, P.J. Tufton, H.C. Webber, M. Healey, *J. Crystal Growth*, v. 24/25, 1974, p. 369.
15. G.A. Satunkin, B.S. Red’kin, V.N. Kurlov, S.N. Rossolenko, V.A. Tatarchenko, Yu.A. Tuffin, *Cryst. Res. & Technol.*, v. 21, 1986, p. 995.
16. V.S. Leibovich, *Bull. Acad. Sci. USSR, Phys. Ser.*, v. 49, 1985, p. 37.
17. G.A. Satunkin, S.N. Rossolenko, V.N. Kurlov, B.S. Red’kin, V.A. Tatarchenko, A.M. Avrutik, *Cryst. Res. & Technol.*, v. 21, 1986, p. 1257.
18. V.V. Voronkov, *Fiz. Tverd. Tela*, v. 5, 1963, p.415 (in Russian).
19. G.A. Satunkin, V.A. Tatarchenko, V.I. Shaitanov, *J. Crystal growth*, v. 50, 1980, p.133.
20. S.N. Rossolenko, *J. Crystal Growth*, v. 231, 2001, p. 306.
21. W. Bardsley, D.T.J. Hurle, G.C. Joyce, *J. Crystal Growth*, v. 40, 1977, p. 13.
22. S.V. Tsvinskii, *Inzh. Fiz. Zh.*, v. 5, 1962, p. 59.
23. T.H. Johansen, *J. Crystal Growth*, v. 80, 1987, p. 343.
24. R. Izermann, “Digital control systems.”, Springer, Berlin, 1981.
25. S.N. Rossolenko, I.S. Pet’kov, V.N. Kurlov, B.S. Red’kin, *J. Crystal Growth*, v. 116, 1992, p. 185.

26. A.V. Zhdanov, S.N. Rossolenko, L.I. Gubina, Proceedings of Stepanov Conference, Ioffe Physico-Technical Institute, Leningrad, 1989, p. 39. (in Russian).
27. M.A. Gevelber, G. Stephanopoulos, M.J. Wargo, *J. Crystal Growth*, v. 91, 1988, p. 199.
28. K. Mika, W. Uelhoff, *J. Crystal Growth*, v. 30, 1975, p. 9.
29. W. Uelhoff, K. Mika, Calculations of shape and stability of menisci in Czochralski growth with tables to determine meniscus maximum heights and capillary constants (Ber. Kernforschungsanlage, Jülich, 1975).
30. B.S. Red'kin, V.N. Kurlov, I.S. Pet'kov, S.N. Rossolenko, *J. Crystal Growth*, v. 104, 1990, p. 77.
31. I.S. Pet'kov, B.S. Red'kin, *J. Crystal Growth*, v. 131, 1993, p. 598.
32. B.S. Red'kin, V.N. Kurlov, I.S. Pet'kov, S.N. Rossolenko, *Ferroelectrics*, v. 133, 1992, p. 289.
33. J.P. Dismukes, L. Ekstrom, *Trans. Met. Soc. AIME*, v.233, 1965 p.672.
34. J.P. Dismukes, W.M. Yim, *J. Crystal Growth*, v. 22, 1974, p.287.
35. N.V. Abrosimov, S.N. Rossolenko, V. Alex, A. Gerhardt, W. Schröder, *J. Crystal Growth*, v.166, 1996, p. 657.
36. N.V. Abrosimov, S.N. Rossolenko, W. Thieme, A. Gerhardt, W. Schröder, *J. Crystal Growth*, v.174, 1997, p.182.
37. A. Erko, F. Schäfers, W. Gudat, N.V. Abrosimov, S.N. Rossolenko, V. Alex, S. Groth, W. Schröder, *Nucl. Instr. and Meth.*, v.A374, 1996, p.408.
38. S. Keitel, C.C. Retsch, T. Niemöller, J.R. Schneider, N.V. Abrosimov, S.N. Rossolenko, H. Riemann, *Nucl. Instr. and Meth.*, v. A414, 1998, p.427.
39. P. Laporte, N.V. Abrosimov, P. Bastie, B. Cordier, G. DiCocco, J. Evrard, L. Gizzi, B. Hamelin, P. Jean, Ph. Laurent, P. Paltani, G.K. Skinner, R.K. Smither, P.vonBallmoos, *Nucl. Instr. and Meth.*, v. A 442, 2000, p. 438.
40. W. Bardsley, D.T.J. Hurle, G.C. Joyce, G.C. Wilson, *J. Crystal Growth*, v.40, 1977, p.21.
41. D.T.J. Hurle, *Crystal pulling from the melt* (Springer-Verlag, Berlin Heidelberg,1993) ch.8, p.97.
42. G.C. Joyce, D.T.J. Hurle, Q.A.E. Vaughan, *J. Crystal Growth*, v.132, 1993, p.1.
43. A. Dahlen, A. Fattah, G. Hanke, E. Karthaus, *Cryst. Res. & Technol.*, v.29, 1994, p.187.
44. I. Yonenaga, A. Matsui, S. Tozawa, K. Sumino, T. Fukuda, *J. Crystal Growth*, v.139, 1995, p.257.
45. D.A. Petrov, *Izv. AN SSSR, Otd. techn. nauk*, v.11, 1956, p.82 (in Russian).
46. G.V. Nikitina, V.N. Romanenko, *Izv. Akad. Nauk SSSR, Neorg. Mater.*, v.3, 1967, p. 1577 (in Russian).
47. H.E. LaBelle, Jr., A.I. Mlavsky, *Nature*, v. 216, No 3115, 1967, p. 574.
48. A.V. Stepanov "The Future of Metalworking" (Lenizdat, Leningrad, 1963) (in Russian).
49. R.E. Novak, R. Metzl, A. Dreeben, S. Berkman, D.L. Patterson, *J. Crystal Growth*, v. 50, 1980, p. 143.

50. K. Wada, K. Hoshikawa, *J. Crystal Growth*, v. 50, 1980, p. 151.
51. E.R. Dobrovinskaya, L.A. Litvinov, V.V. Pishchik, *J. Crystal Growth*, v. 50, 1980, p. 341.
52. D. Nicoara, I. Nicoara, *J. Crystal Growth*, v. 82, 1987, p. 95.
53. V.A. Tatarchenko, T.N. Yalovets, G.A. Satunkin, L.M. Zatulovsky, L.P. Egorov, D.Ya. Kravetsky, *J. Crystal Growth*, v. 50, 1980, p. 335.
54. V.N. Kurlov, S.N. Rossolenko, *J. Crystal Growth*, v. 173, 1997, p. 417.
55. V.N. Kurlov, B.M. Epelbaum, *J. Crystal Growth*, v. 187, 1998, p. 107.
56. M.V. Klassen-Neklyudova, Kh.S. Bagdasarov (Eds.), “Ruby and Sapphire” Nauka, Moscow, 1974 (in Russian).
57. V.N. Kurlov, S.N. Rossolenko, *Bull. Rus. Acad. Sci., Physics*, v. 63, No 9, 1999, p. 1339.
58. V.V. Voronkov, *Bull. Acad. of Sci. USSR, Phys. Ser.*, v. 47, 1983, p. 1.
59. V.N. Kurlov, B.M. Epelbaum, S.N. Rossolenko, *Bull. Rus. Acad. Sci., Physics*, v. 63, No 9, 1999, p. 1705.
60. V.N. Kurlov, S.N. Rossolenko, *Bull. Rus. Acad. Sci., Physics*, v. 63, No 9, 1999, p. 1711.
61. V.N. Kurlov, *J. Crystal Growth*, v. 179, 1997, p. 168.
62. V.N. Kurlov “Sapphire: Properties, Growth, and Applications.” - *Encyclopedia of Materials: Science and Technology*, Ed. by K.H.J. Buschow et al. Published by Elsevier Science under the Pergamon imprint, 2001, p. 8259.
63. P.I. Antonov, V.N. Kurlov, *Progress in Crystal Growth and Characterization of Materials*, v. 44, 2002, p. 63.



Dr. Nikolai V. Abrosimov graduated from the Nizhny Novgorod State University in 1975. Then he joined the Institute of Solid State Physics, Russian Academy of Science where he worked up to the present. He was engaged among other things in shaped silicon crystal growth, flux-growth of high temperature superconductor single crystals and their characterization. Since 1993 he works also as a guest scientist in the Institute of Crystal Growth, Berlin, Germany engaged in the Czochralski growth of silicon-germanium single crystals and development of novel growth techniques.



Dr. Vladimir Kurlov was educated at the M.V.Lomonosov Moscow Institute of Fine Chemical Technology in 1982, where he obtained MSc in technology of special materials for electronics. Then he joined the Institute of Solid State Physics, Russian Academy of Sciences where he worked up to the present. He was engaged in crystal growth from the melt. He received a Ph.D. degree in Solid State Physics in 1992 in the Institute of Solid State Physics. Dr V.N. Kurlov is the author of over 50 research papers and reviews concerning the crystal growth from the melt.

Dr. Sergei Rossolenko graduated from the Moscow Institute of Microelectronics in 1983 where he obtained a degree of MSc in automatics for microelectronic equipment. Then he entered the Institute of Solid State Physics of Russian Academy of Sciences where he works up to the present. He was engaged in automatization and mathematical modelling of the processes of the crystal growth from the melt. He received a Ph.D. degree in the area of Solid State Physics in 1988 in the Institute of Solid State Physics. Dr. S. Rossolenko is the author of over 20 research papers relating to the automatization and mathematical modelling of crystal growth from the melt.